marine drugs

MDPI

*Supporting Information*

# Applying a Chemogeographic Strategy for Natural Product Discovery from the Marine Cyanobacterium *Moorena bouillonii*

**Christopher A. Leber [1], C. Benjamin Naman[1,2], Lena Keller[1,3], Jehad Almaliti[1,4], Eduardo J. E. Caro-Diaz[1,5], Evgenia Glukhov[1], Valsamma Joseph[1,6], T. P. Sajeevan[1,6], Andres Joshua Reyes[7], Jason S. Biggs[7], Te Li[2], Ye Yuan[2], Shan He[2], Xiaojun Yan[2], and William H. Gerwick [1,8,*]**

[1] Center for Marine Biotechnology and Biomedicine, Scripps Institution of Oceanography, University of California San Diego, La Jolla, California 92093, United States; cleber@ucsd.edu (C.A.L.); bnaman@nbu.edu.cn (C.B.N.); le.keller85@gmail.com (L.K.); jalmaliti@ucsd.edu (J.A.); eduardo.caro1@upr.edu (E.J.E.C.D.); eglukhov@ucsd.edu (E.G.); valsamma@cusat.ac.in (V.J.); sajeev@cusat.ac.in (T.P.S.)

[2] Li Dak Sum Yip Yio Chin Kenneth Li Marine Biopharmaceutical Research Center, Department of Marine Pharmacy, College of Food and Pharmaceutical Sciences, Ningbo University, Ningbo, China; telinbu@163.com (T.L.); 23yuanye@163.com (Y.Y.); heshan@nbu.edu.cn (S.H.); yanxiaojun@nbu.edu.cn (X.Y.)

[3] Department Microbial Natural Products, Helmholtz-Institute for Pharmaceutical Research Saarland (HIPS), Helmholtz Centre for Infection Research (HZI), Campus E8.1, 66123 Saarbrücken, Germany

[4] School of Pharmacy, The University of Jordan, Amman, Jordan

[5] Department of Pharmaceutical Sciences, School of Pharmacy, University of Puerto Rico – Medical Sciences Campus, San Juan, Puerto Rico 00921

[6] National Centre for Aquatic Animal Health, Cochin University of Science and Technology, Kochi, Kerala 682016, India

[7] University of Guam Marine Laboratory, Mangilao, Guam 96923; reyes.andresjoshua@gmail.com (A.J.R.); biggs.js@gmail.com (J.S.B.)

[8] Skaggs School of Pharmacy and Pharmaceutical Sciences, University of California San Diego, La Jolla, California 92093, United States

* Correspondence: wgerwick@health.ucsd.edu (W.H.G.)

Received: XX; Accepted: XX; Published: XX

## Table of Contents

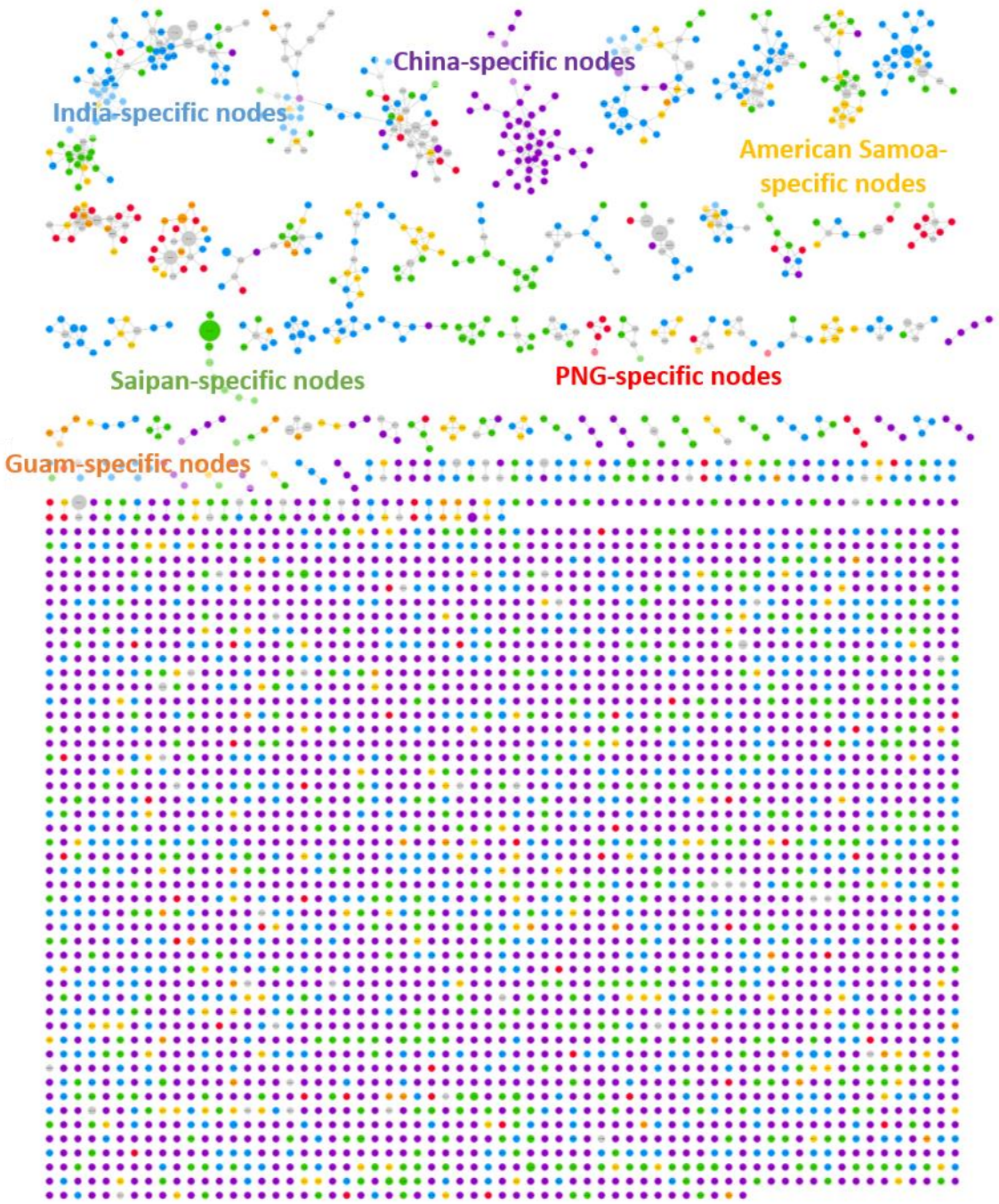


**Figure S1.** Molecular network of M. bouillonii crude extracts

GNPS classical molecular network of *M. bouillonii* crude extracts showing clusters of regionally specific nodes. Grey nodes represent $MS^2$ features that are present in samples from more than one geographically region. Nodes are scaled to summed precursor intensity. Red: Papua New Guinea, Orange: Guam, Gold: American Samoa, Green: Saipan, Blue: Kavaratti (Lakshadweep Islands, India), Purple: Xisha (Paracel) Islands in the South China Sea. See Table S9 for network parameters.

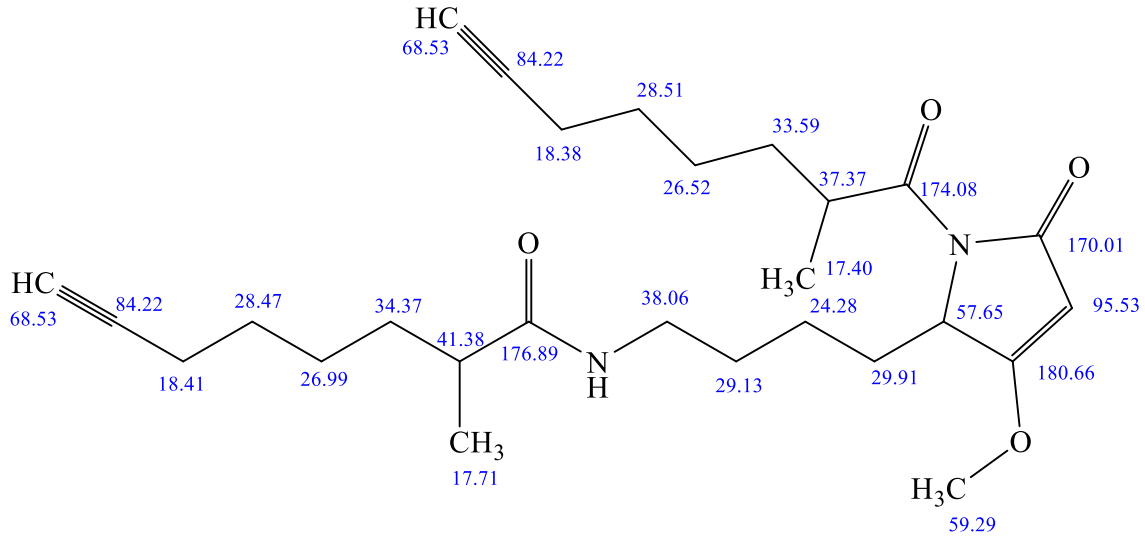


**Figure S2.** Predicted $^{13}C$ shifts for candidate structure **1a**

$^{13}C$ NMR shifts were calculated using ACD/Labs 2019.2.1 (ACD/C+H Predictors and DB 2019.2.1) (https://www.acdlabs.com/index.php).

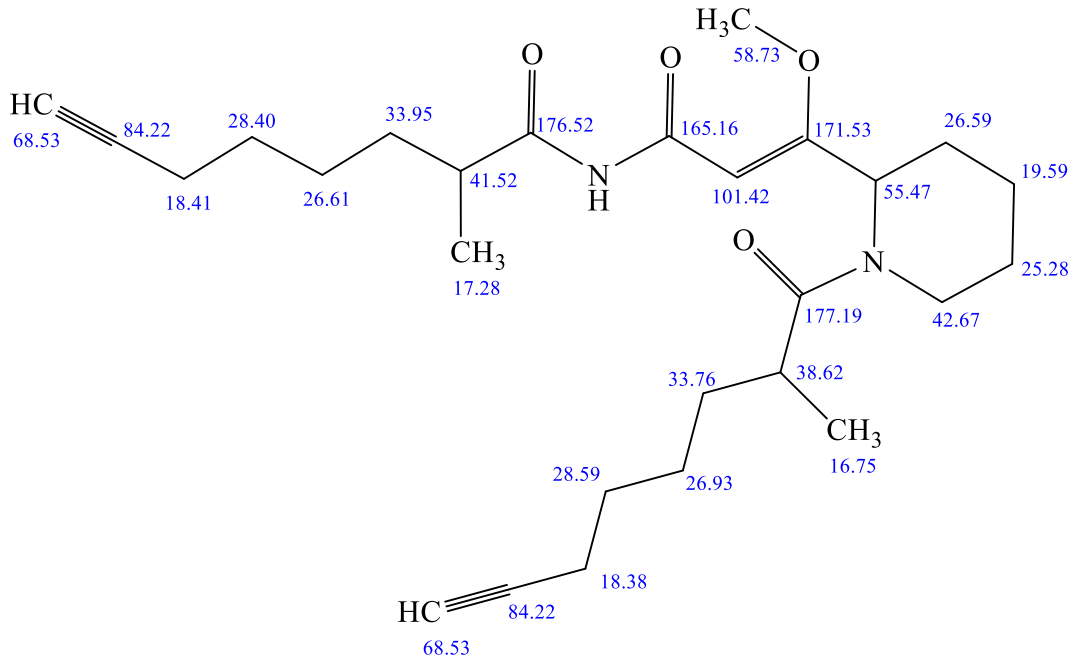


**Figure S3.** Predicted $^{13}C$ shifts for candidate structure **1b**

$^{13}C$ NMR shifts were calculated using ACD/Labs 2019.2.1 (ACD/C+H Predictors and DB 2019.2.1) (https://www.acdlabs.com/index.php).

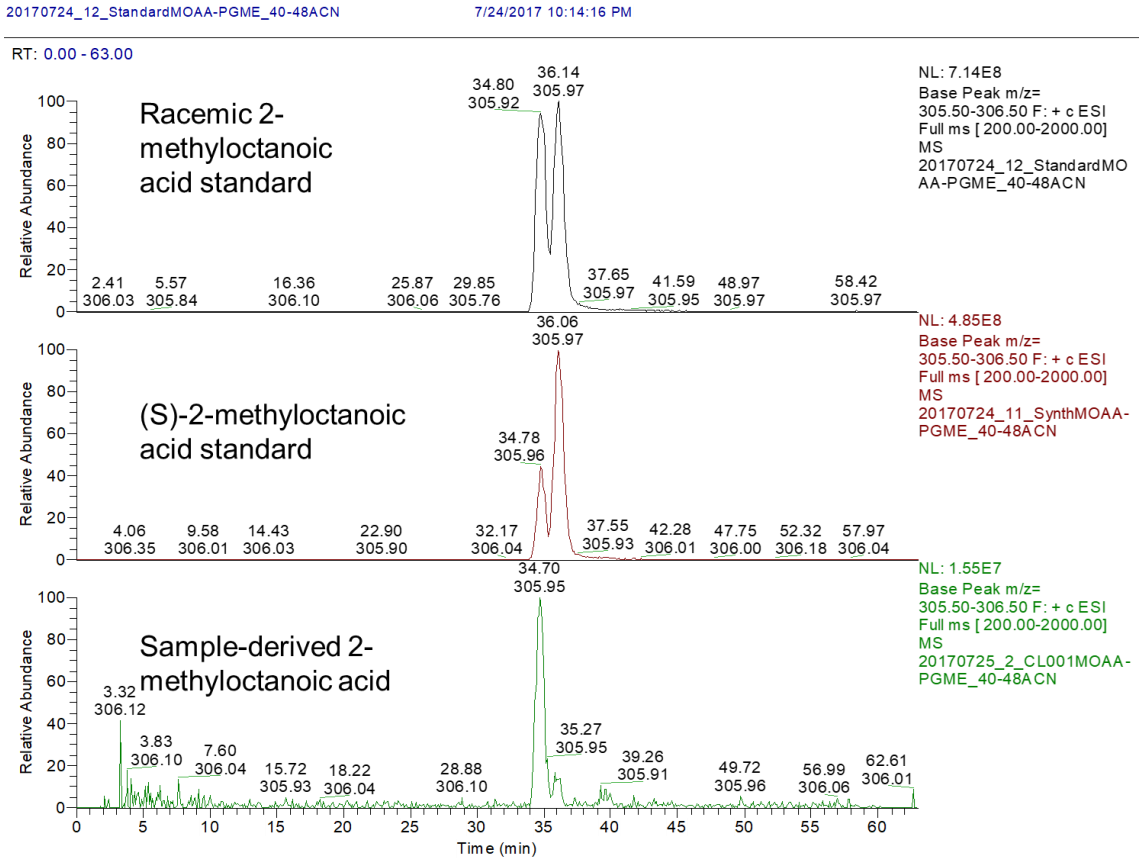


**Figure S4.** Compound **1** derived 2-methyoctanoic acid compared to standards
LC-MS TIC traces comparing (*S*)-(+)-2-phenylglycine methyl ester derivatized racemic 2-methyloctanoic acid and (*S*)-2-methyloctanoic acid standards to sample-derived 2-methyl octanoic acid, indicating the sample-derived 2-methyl octanoic acid to be of the *R* configuration.

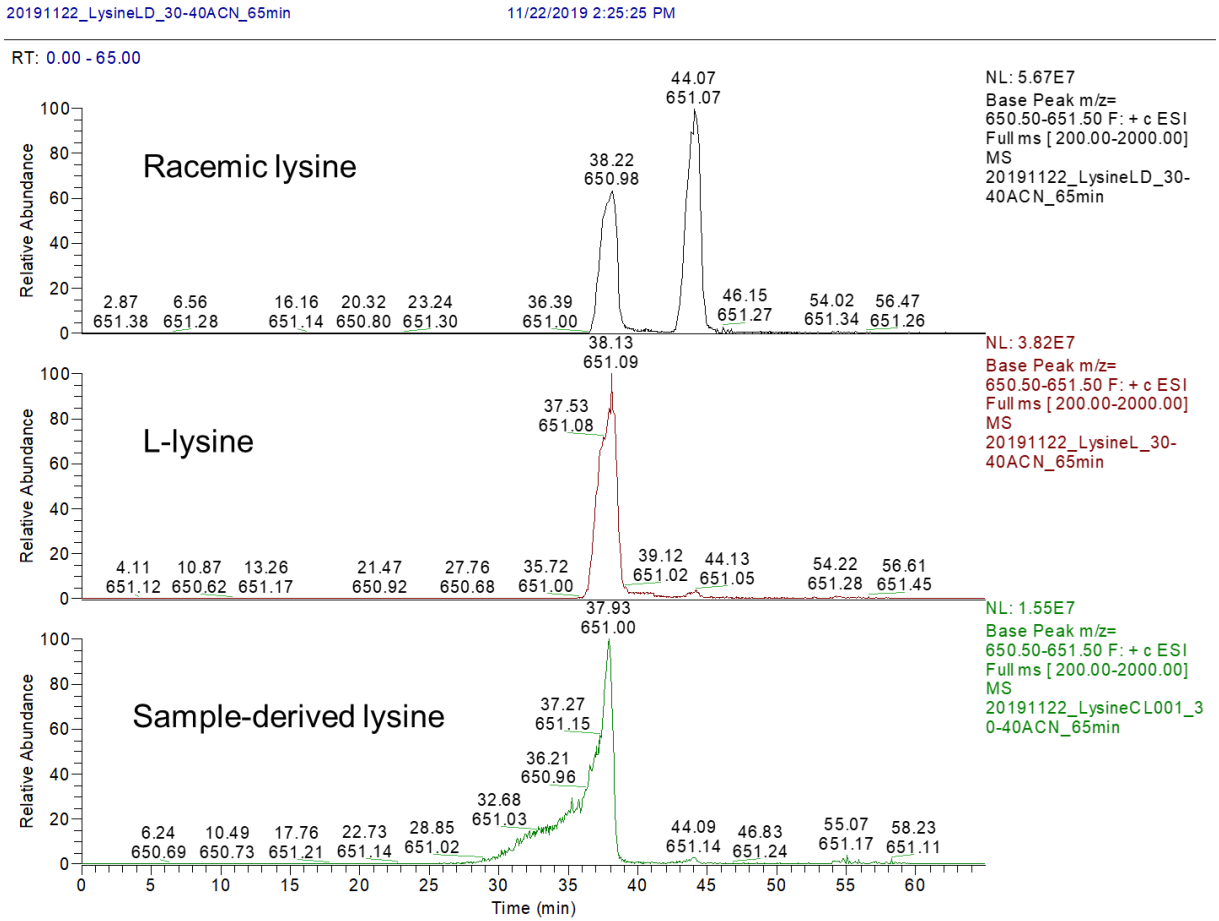


**Figure S5.** Compound **1** derived lysine compared to standards

LC-MS TIC traces comparing L-FDAA derivatized racemic lysine and L-lysine standards to sample-derived lysine, indicating the sample-derived lysine to be of the *S* configuration (L-lysine).

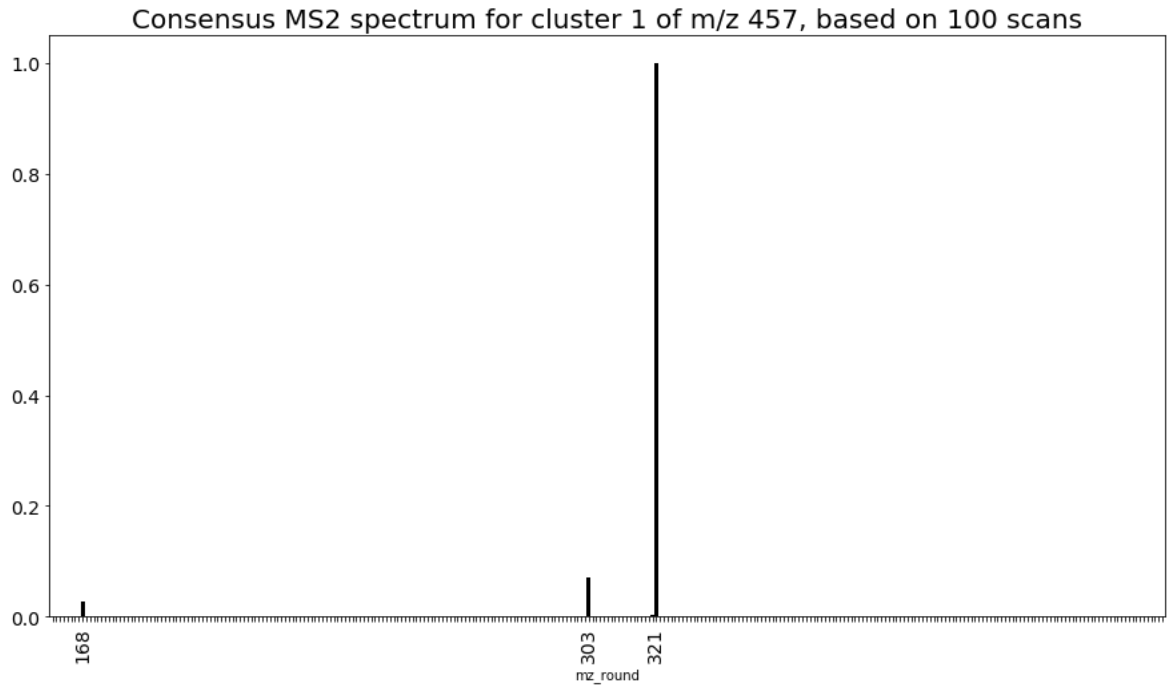


**Figure S6.** Doscadenamide A (**1**) consensus $MS^2$ spectrum

Consensus $MS^2$ spectrum representing a cluster of 100 scans for precursor mass *m*/*z* 457 and displaying the fragmentation spectrum for doscadenamide A (**1**).

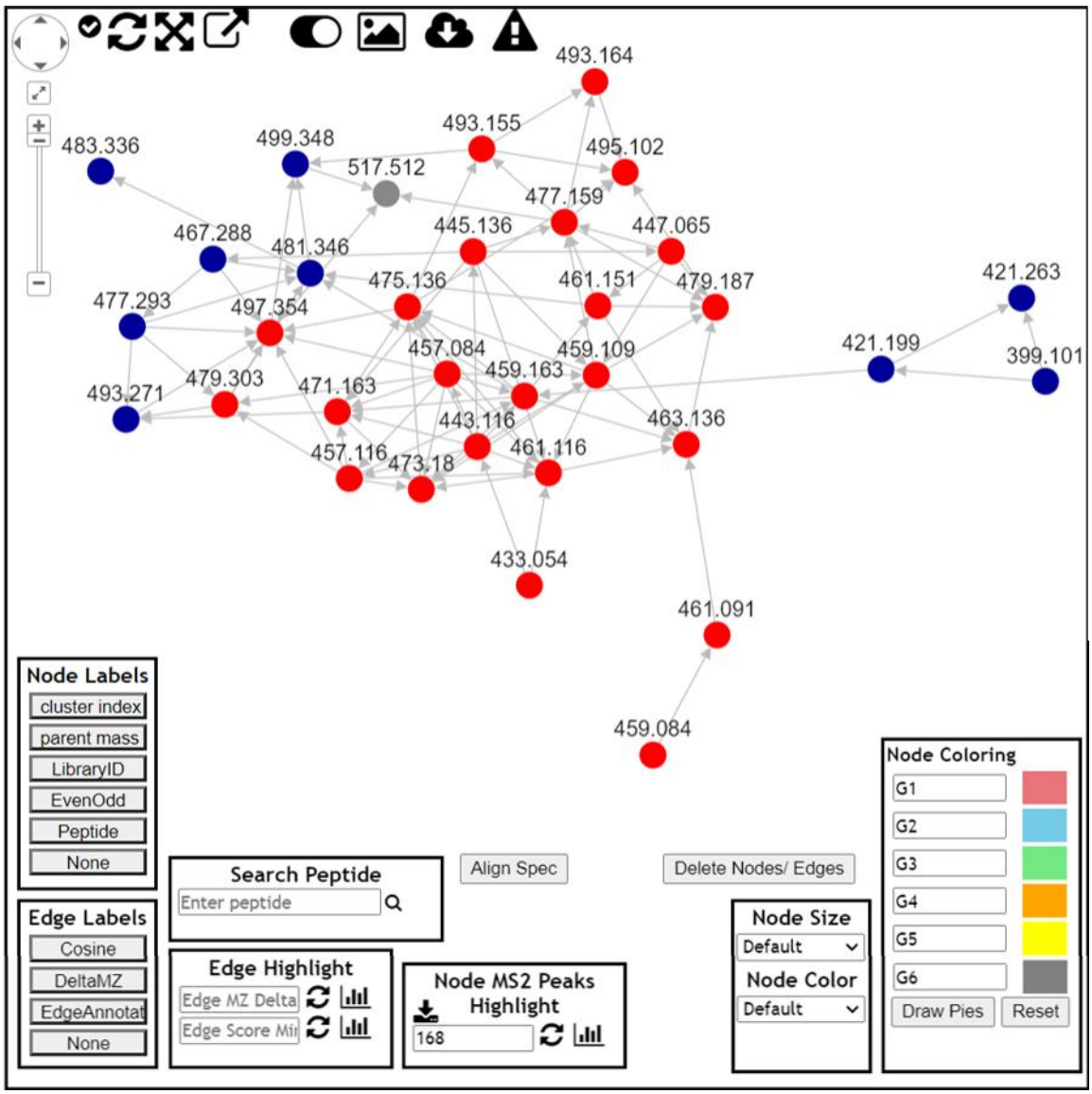


**Figure S7.** Molecular network cluster of compound **1** and analogs, highlighting *m*/*z* 168 frag. peak

A cluster of 33 $MS^2$ spectral nodes, including compound **1** (*m*/*z* 457.084), as visualized in the GNPS in browser network visualizer. This cluster is a part of a GNPS classical molecular network generated with crude extracts and fractions from two *M. bouillonii* samples: one from Saipan and one from Guam. All nodes colored red (23 out of 33) possess a fragment peak at *m*/*z* 168, suggesting that the structures they represent include a heterocyclic core identical to compound **1**.

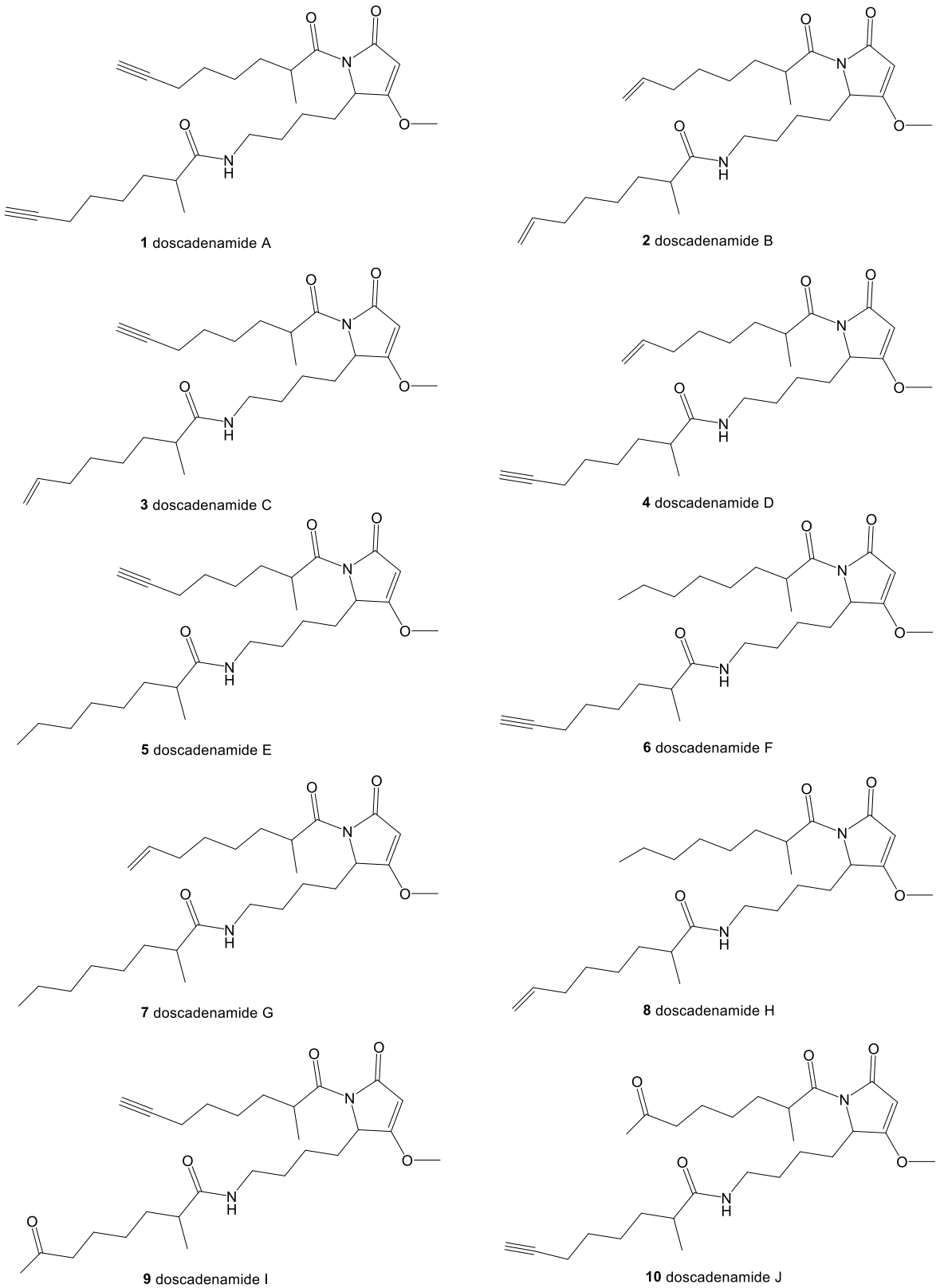


**Figure S8.** Structure of compound **1** with structure proposals for analogs (**2-10**)
The doscadenamides: compound **1**, along with analogs whose proposed structures were annotated via informative patterns in the $MS^2$ fragmentation data (See Figures S9-S26).

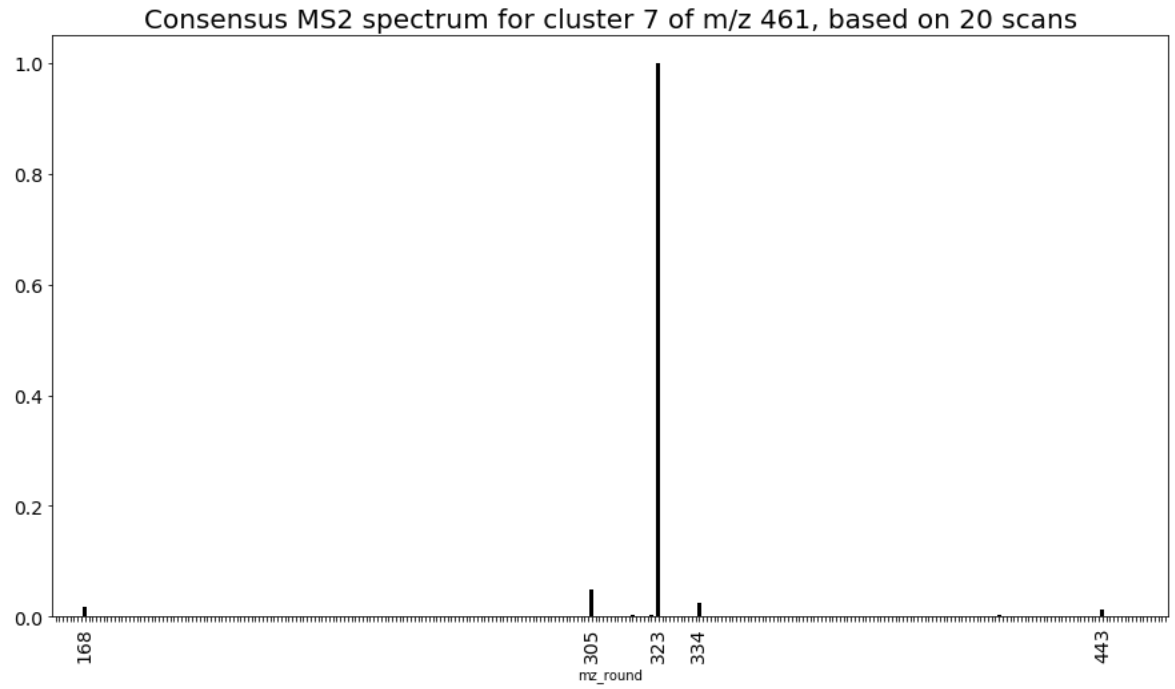


**Figure S9.** Doscadenamide B (**2**) consensus $MS^2$ spectrum

Consensus $MS^2$ spectrum representing a cluster of 20 scans for precursor mass *m*/*z* 461, representing the fragmentation spectrum of the proposed analog doscadenamide B (**2**).

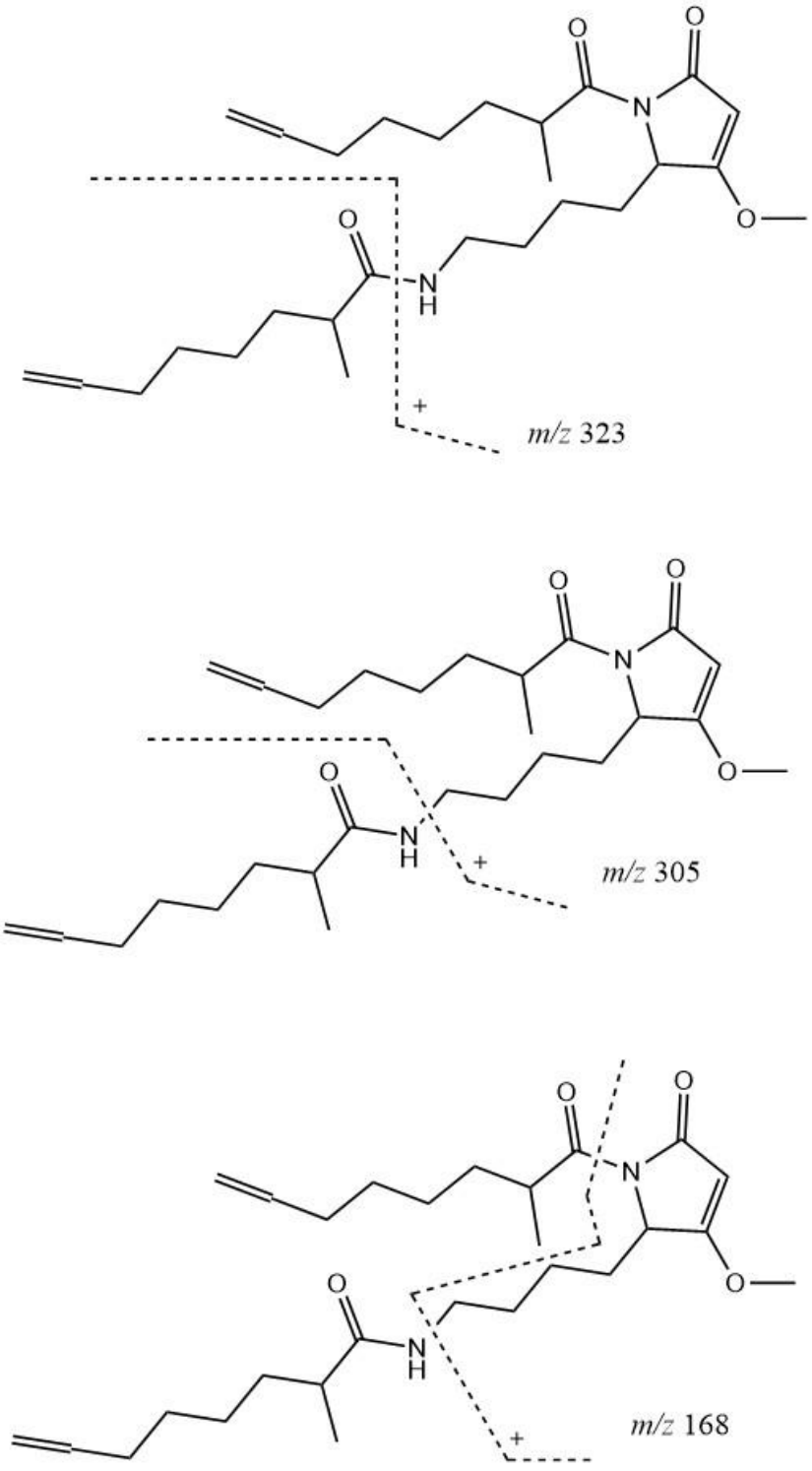


**Figure S10.** Doscadenamide B (**2**) proposed fragmentation

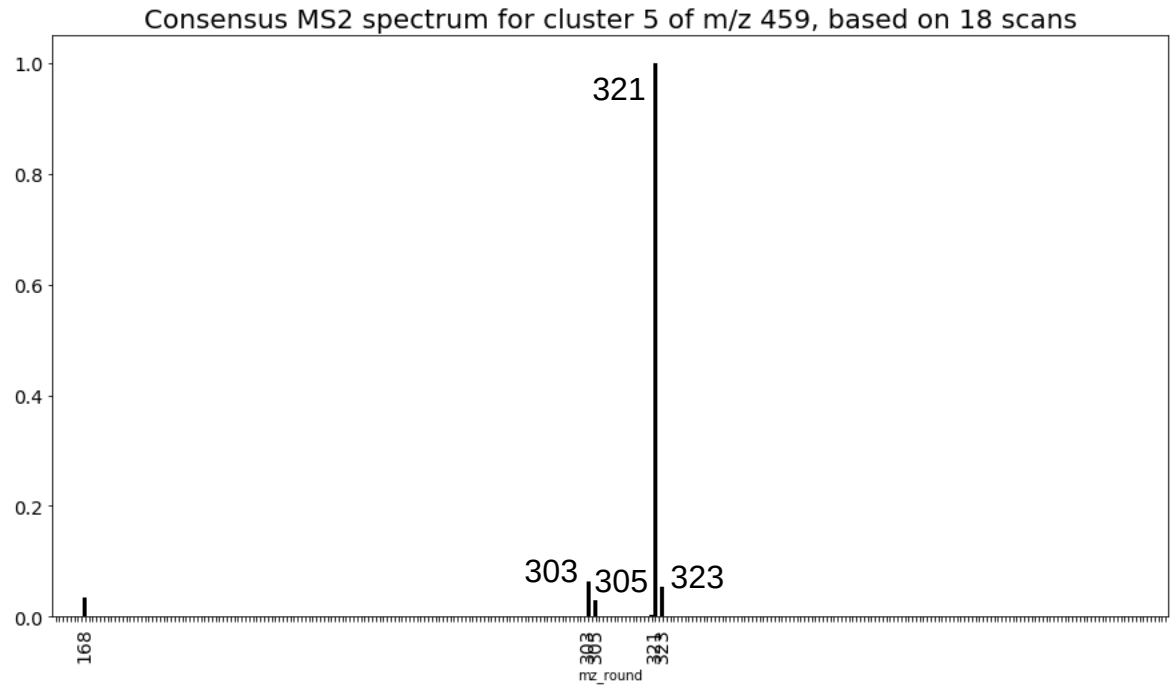


**Figure S11.** Doscadenamide C (**3**) consensus $MS^2$ spectrum

Consensus $MS^2$ spectrum representing a cluster of 18 scans for precursor mass *m*/*z* 459, representing the fragmentation spectrum of the proposed analog doscadenamide C (**3**).

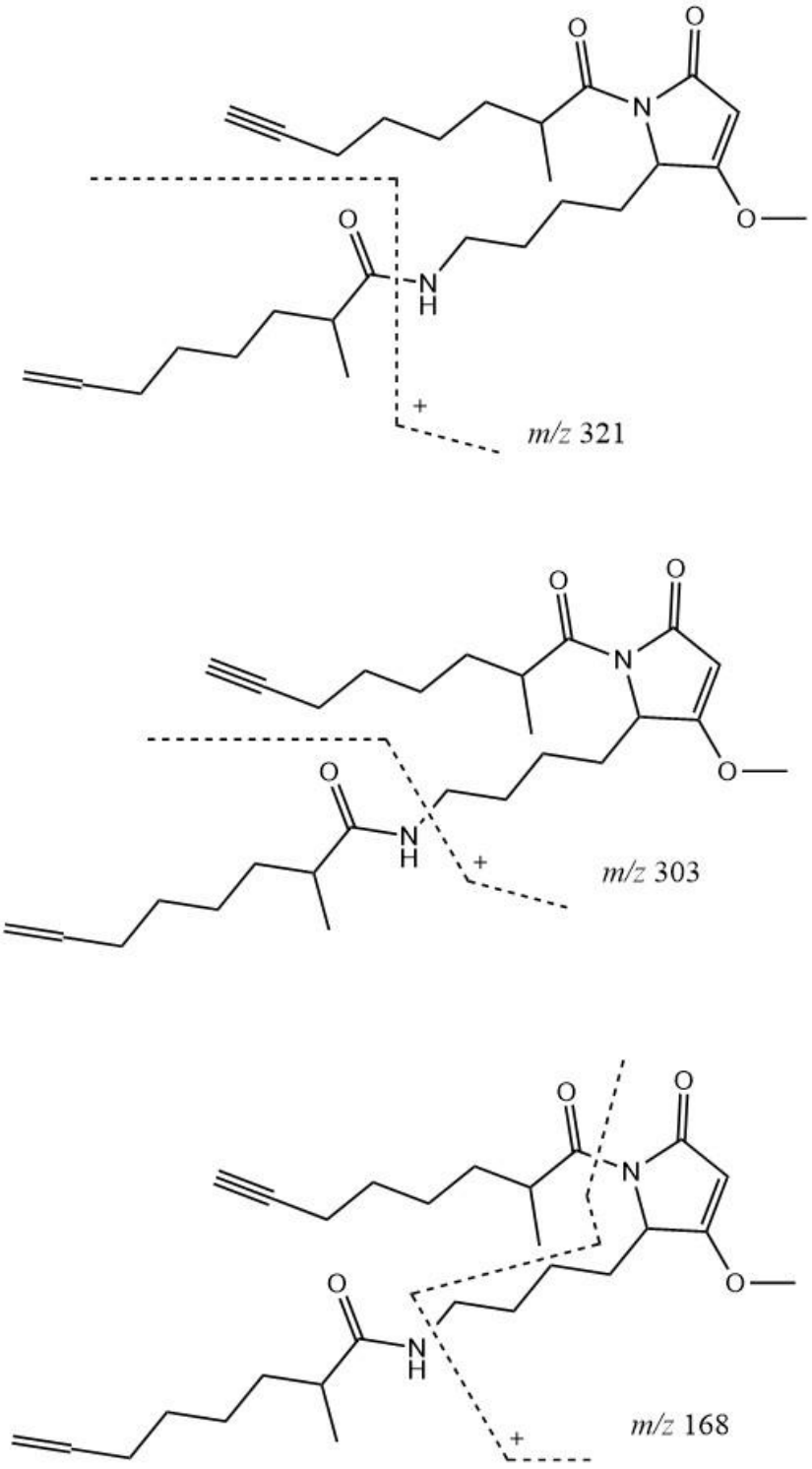


**Figure S12.** Doscadenamide C (**3**) proposed fragmentation

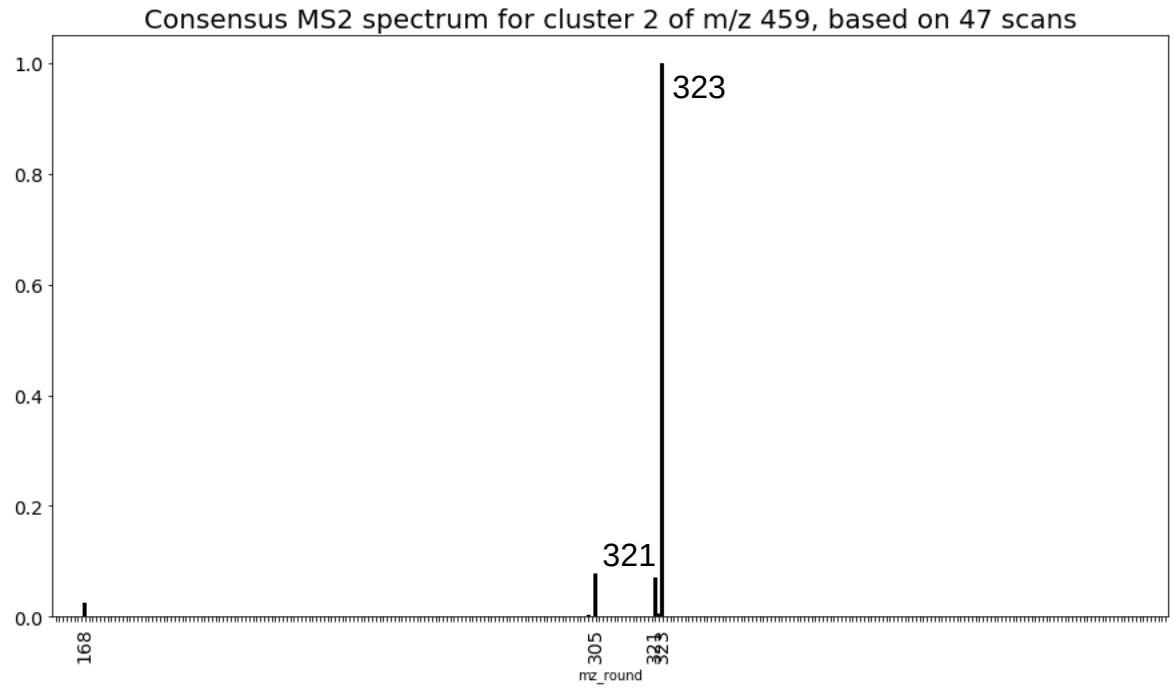


**Figure S13.** Doscadenamide D (**4**) consensus MS² spectrum
Consensus MS² spectrum representing a cluster of 47 scans for precursor mass *m*/*z* 459, representing the fragmentation spectrum of the proposed analog doscadenamide D (**4**).

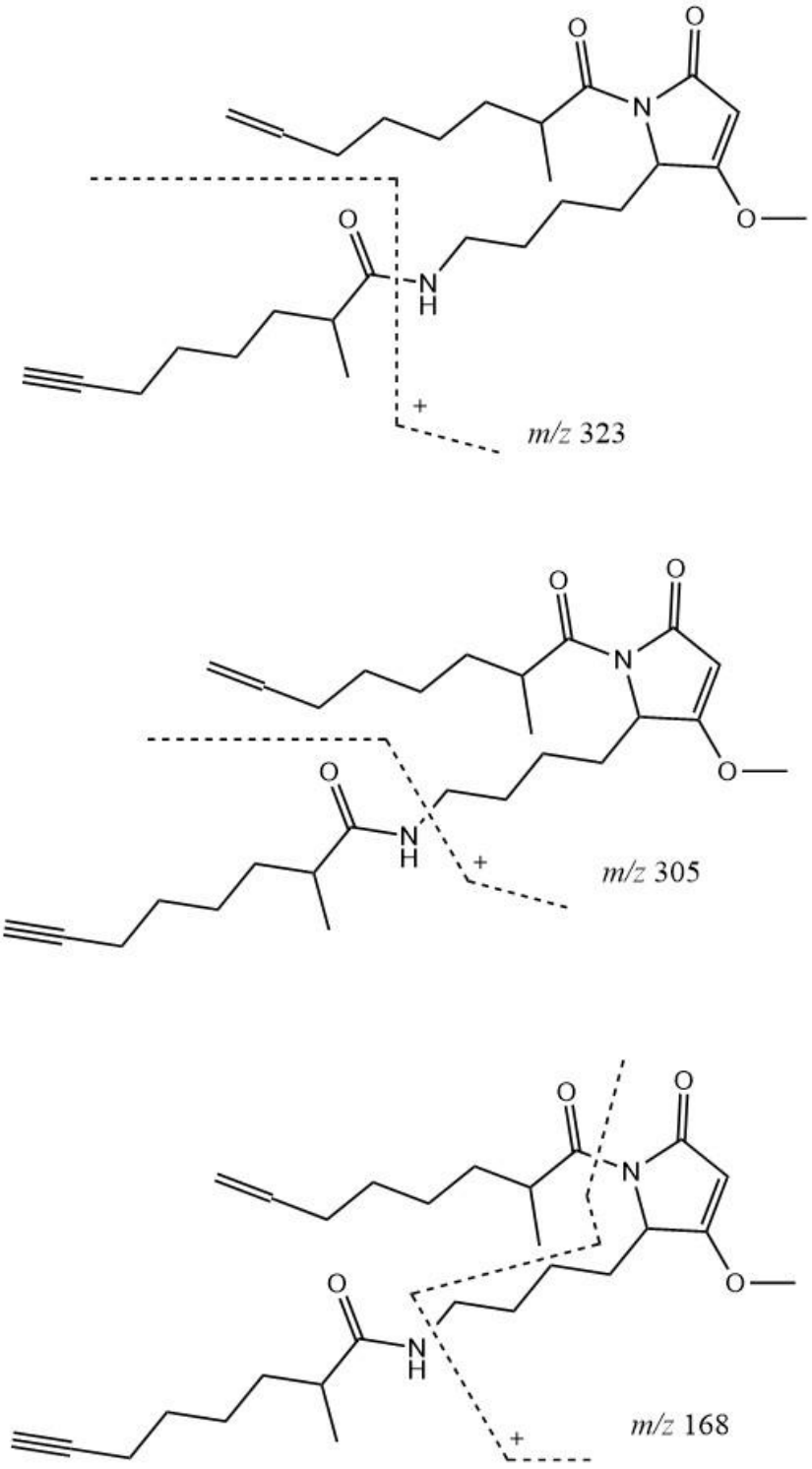


**Figure S14.** Doscadenamide D (**4**) proposed fragmentation

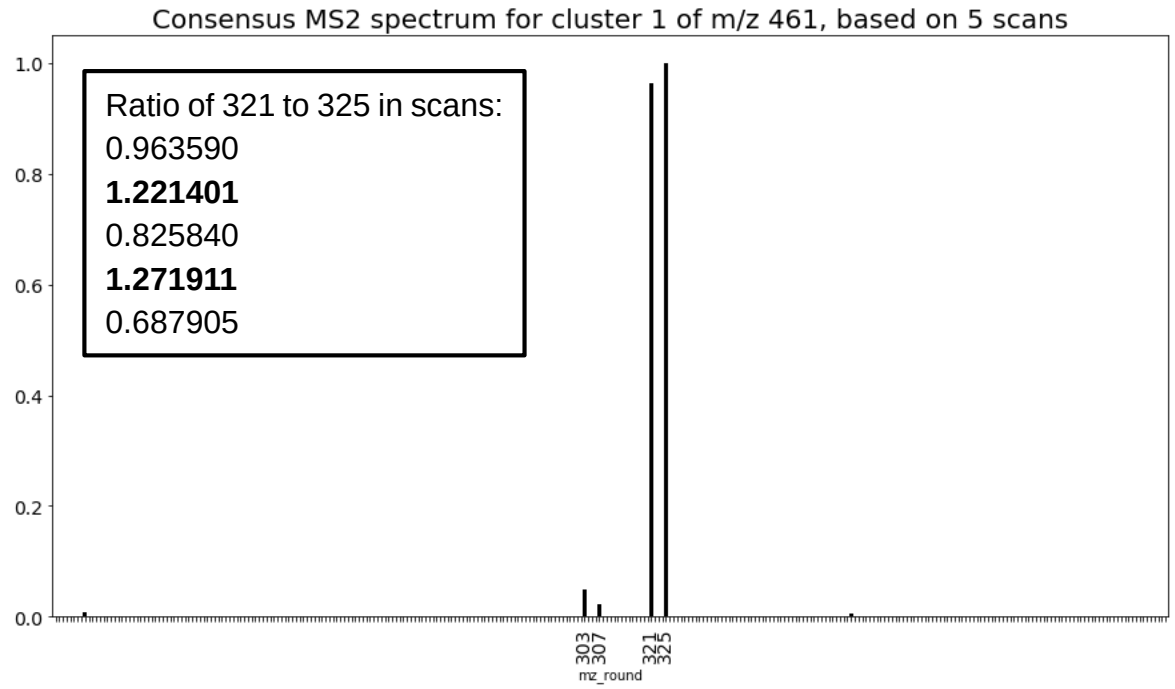


**Figure S15.** Doscadenamide E (**5**) consensus $MS^2$ spectrum

Consensus $MS^2$ spectrum representing a cluster of 5 scans for precursor mass *m*/*z* 461, representing the fragmentation spectrum of the proposed analog doscadenamide E (**5**). The expected fragmentation spectrum would have a fragment peak at *m*/*z* 321 that is more intense than the fragment peak at *m*/*z* 325, indicating the apparent propensity for side chains acylated to the terminus of the lysine side chain to fragment. The inlay in the top right hand corner reports the ratio of the *m*/*z* 321 peak relative intensity to *m*/*z* 325 peak relative intensity for the 5 scans represented in the consensus. These ratios reveal that in 2 scans, the fragment peak at *m*/*z* 321 is indeed more intense than the fragment peak at *m*/*z* 325.

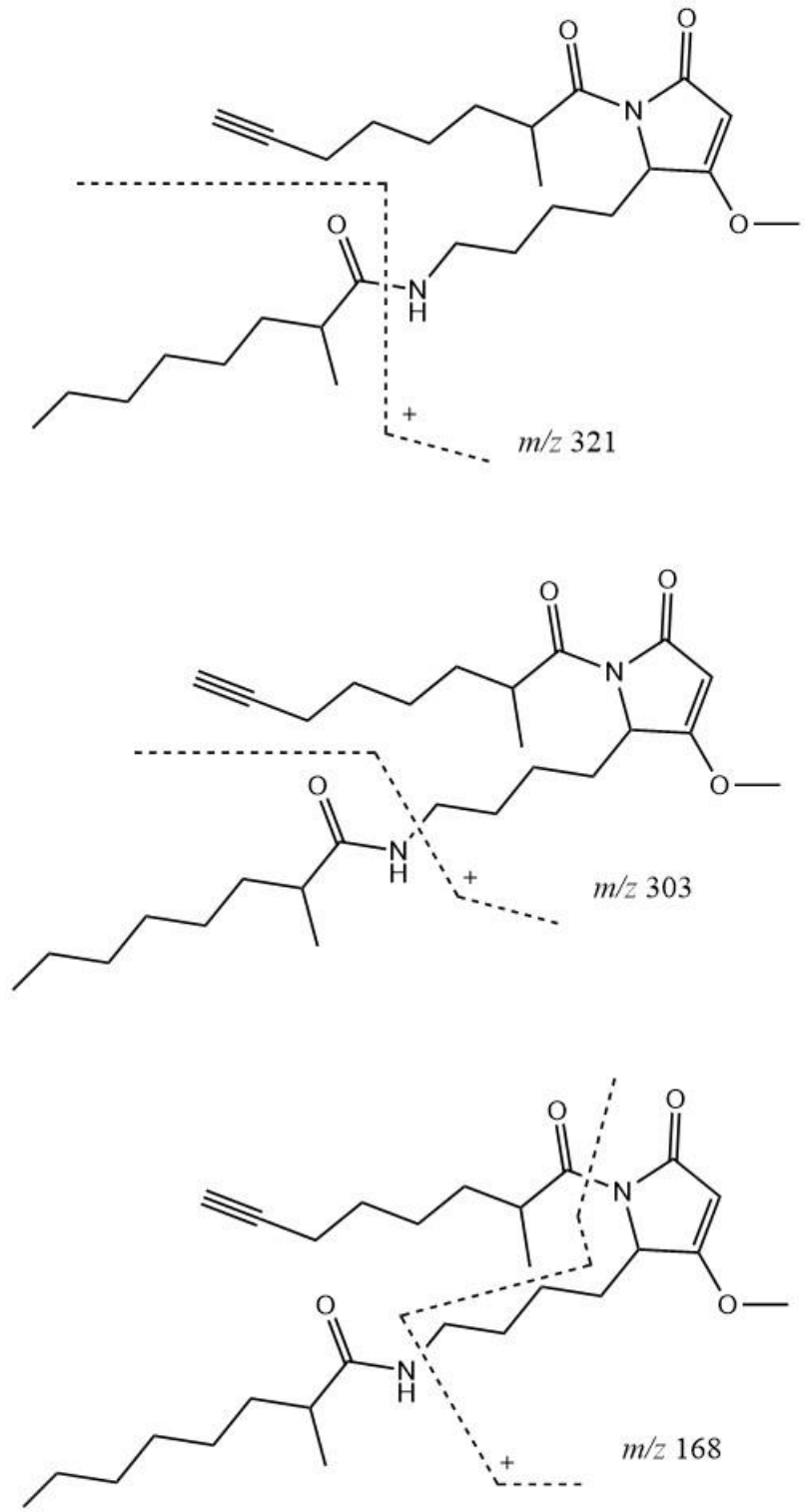


171

172 **Figure S16.** Doscadenamide E (**5**) proposed fragmentation

173

174

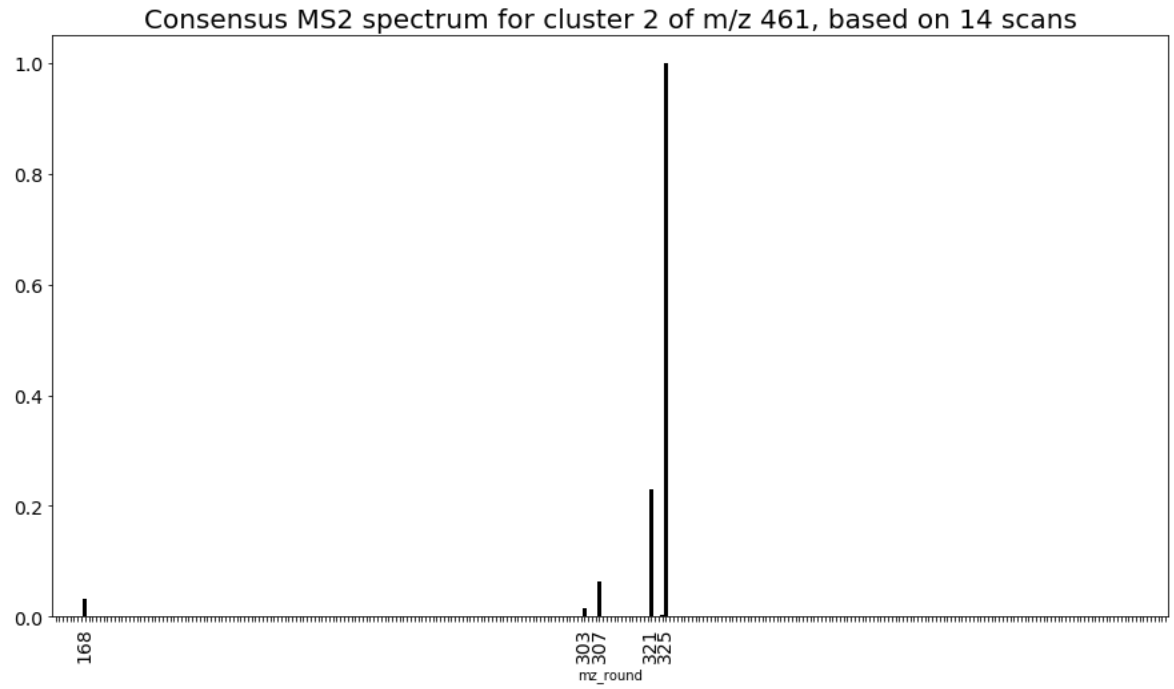


175

176 **Figure S17.** Doscadenamide F (**6**) consensus $MS_2$ spectrum
177 Consensus $MS^2$ spectrum representing a cluster of 14 scans for precursor mass *m*/*z* 461, representing the
178 fragmentation spectrum of the proposed analog doscadenamide F (**6**).

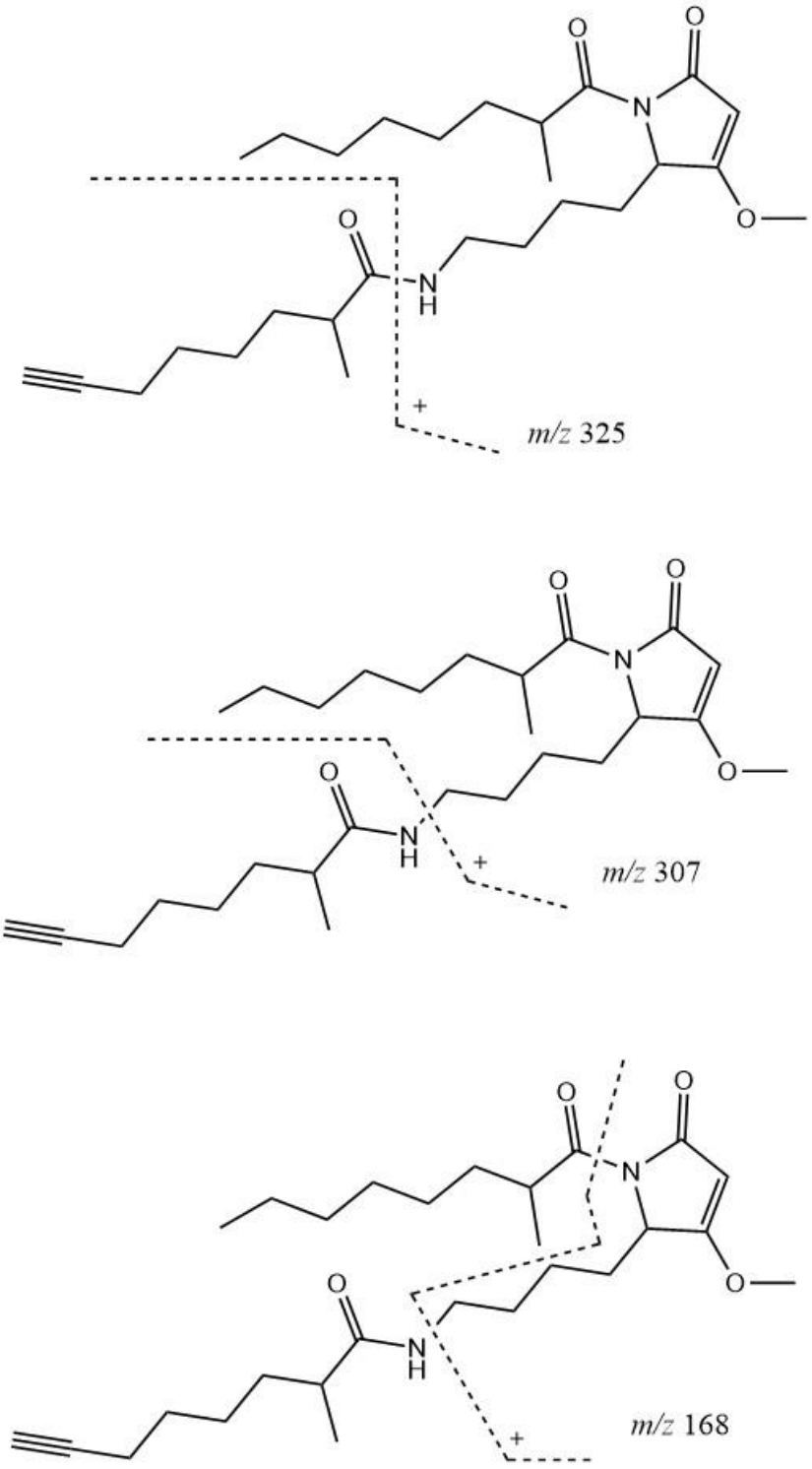


**Figure S18.** Doscadenamide F (**6**) proposed fragmentation

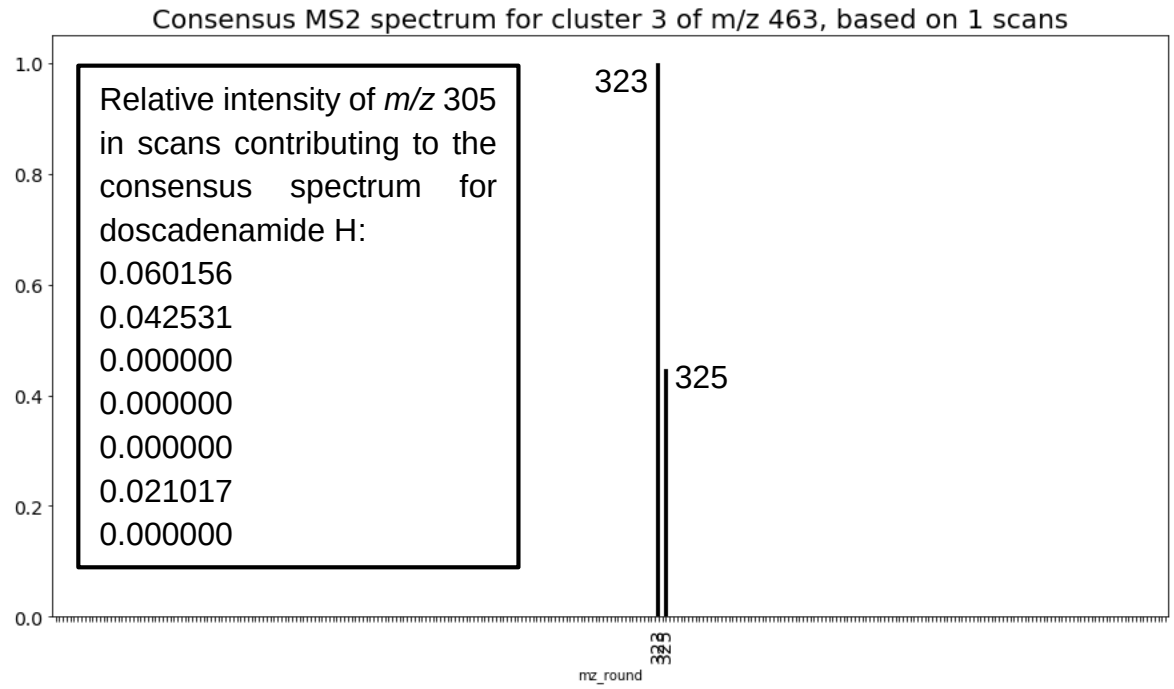


**Figure S19.** Doscadenamide G (**7**) consensus MS$^2$ spectrum

MS$^2$ spectrum captured in one scan for precursor mass *m*/*z* 463, representing the partial fragmentation spectrum of the proposed analog doscadenamide G (**7**). The expected *m*/*z* 305 and *m*/*z* 168 peaks were detected at too low of intensity to appear in this output. However, the *m*/*z* 305 peak is detected in several of the scans that make up the consensus spectrum representing doscadenamide H (Figure S20) – the relative intensity of these *m*/*z* 305 fragment peaks are displayed in the above figure inlay. Detection of this m/z 305 peak is important because doscadenamides G and H coelute and such a fragment peak would not be produced by doscadenamide H. Therefore, this lends further support to the structural proposal for doscadenamide G.

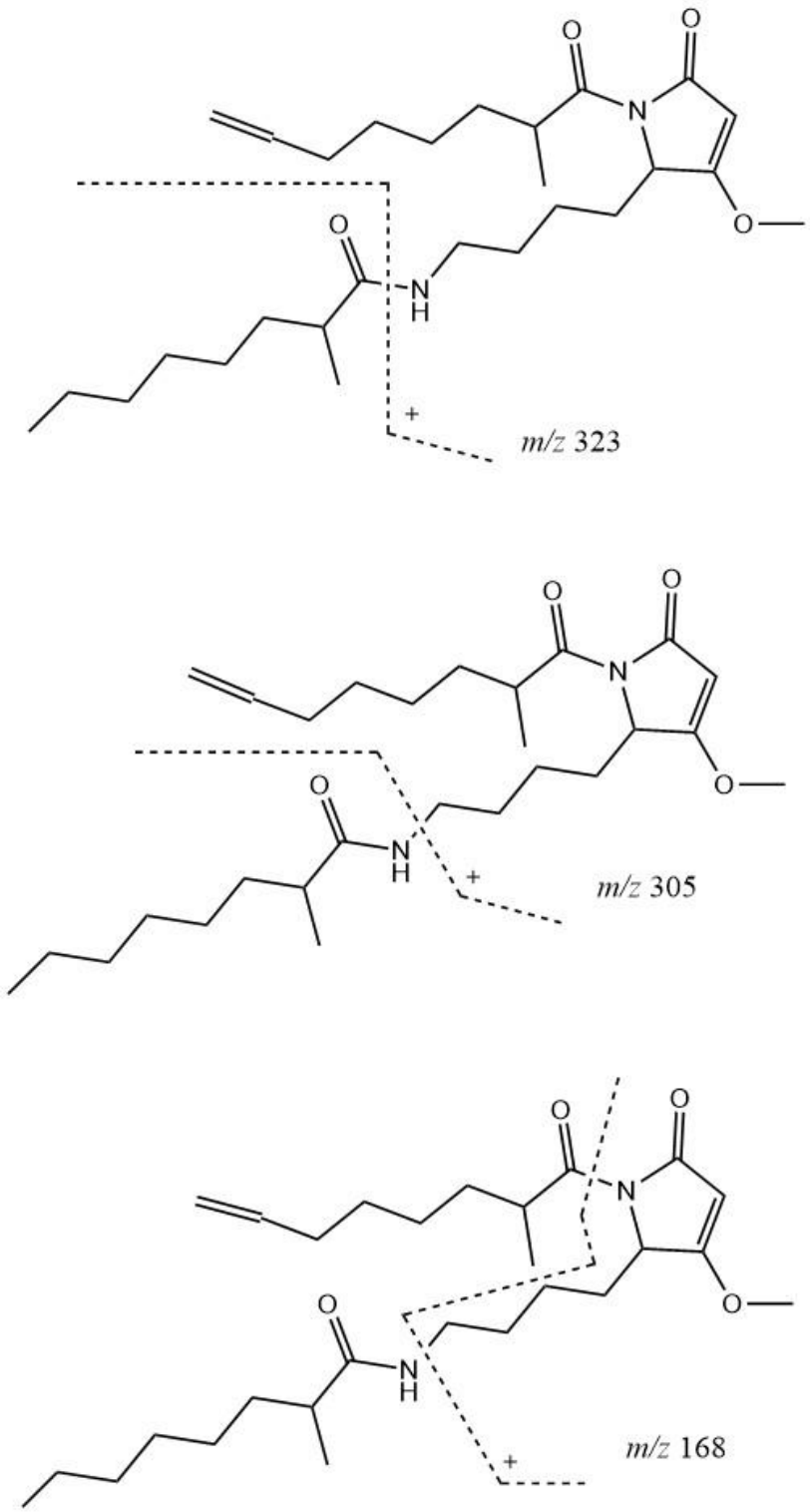


**Figure S20.** Doscadenamide G (**7**) proposed fragmentation

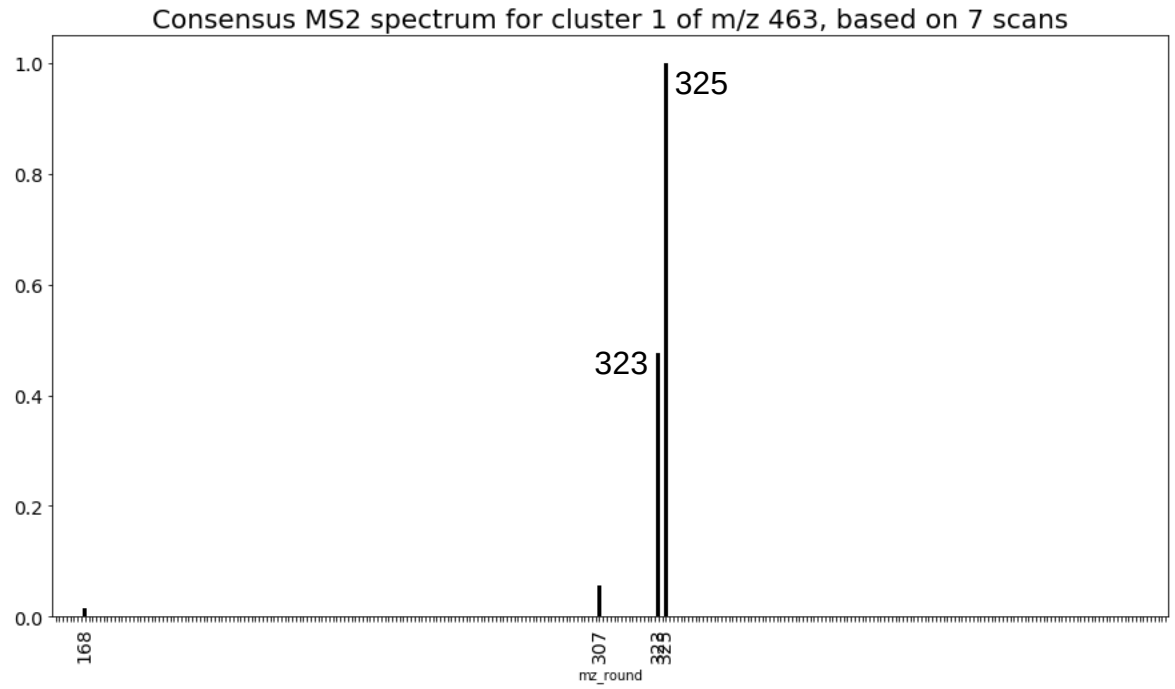


**Figure S21.** Doscadenamide H (**8**) consensus MS² spectrum
Consensus MS² spectrum representing a cluster of 7 scans for precursor mass *m*/*z* 463, representing the fragmentation spectrum of the proposed analog doscadenamide H (**8**).

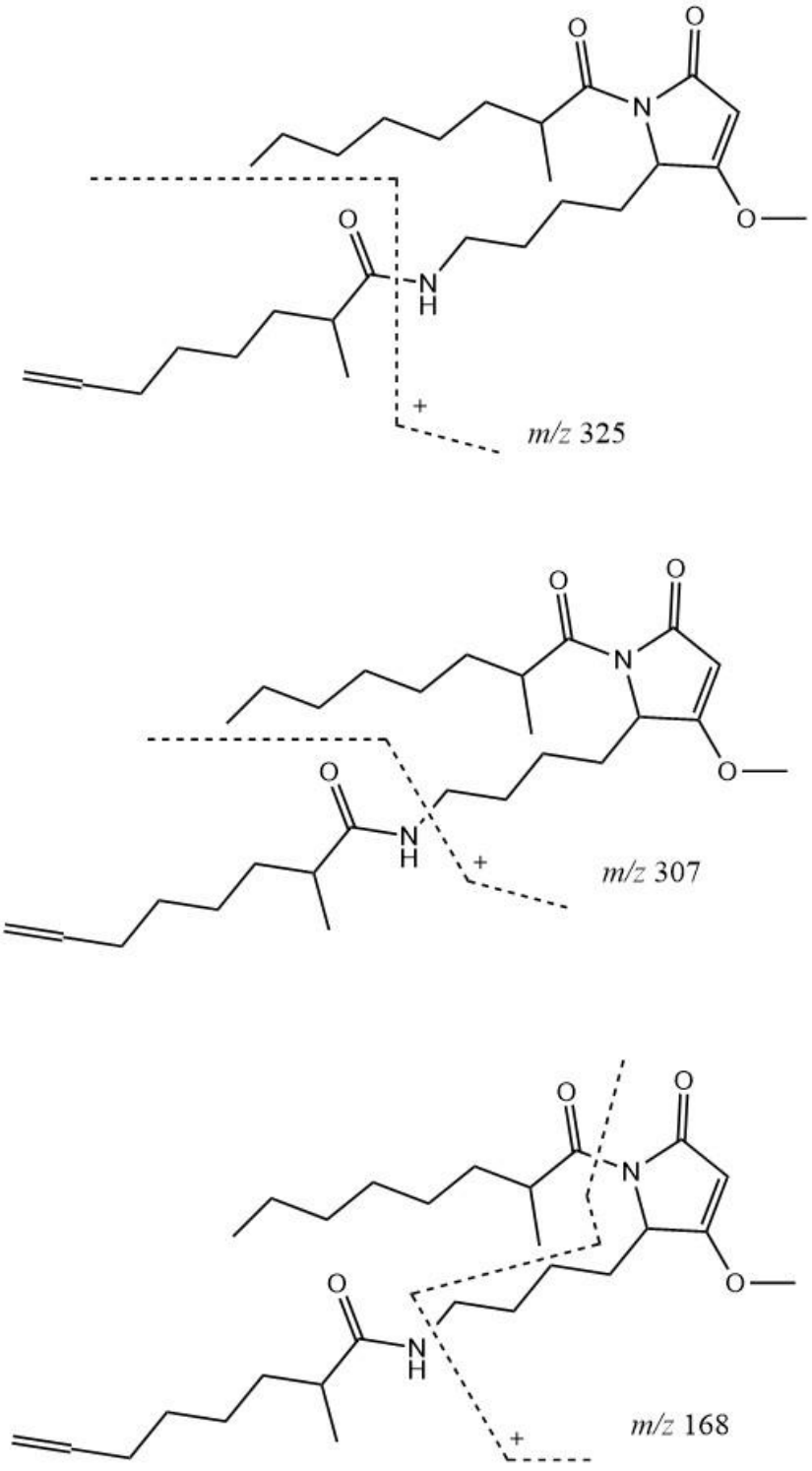


**Figure S22.** Doscadenamide H (**8**) proposed fragmentation

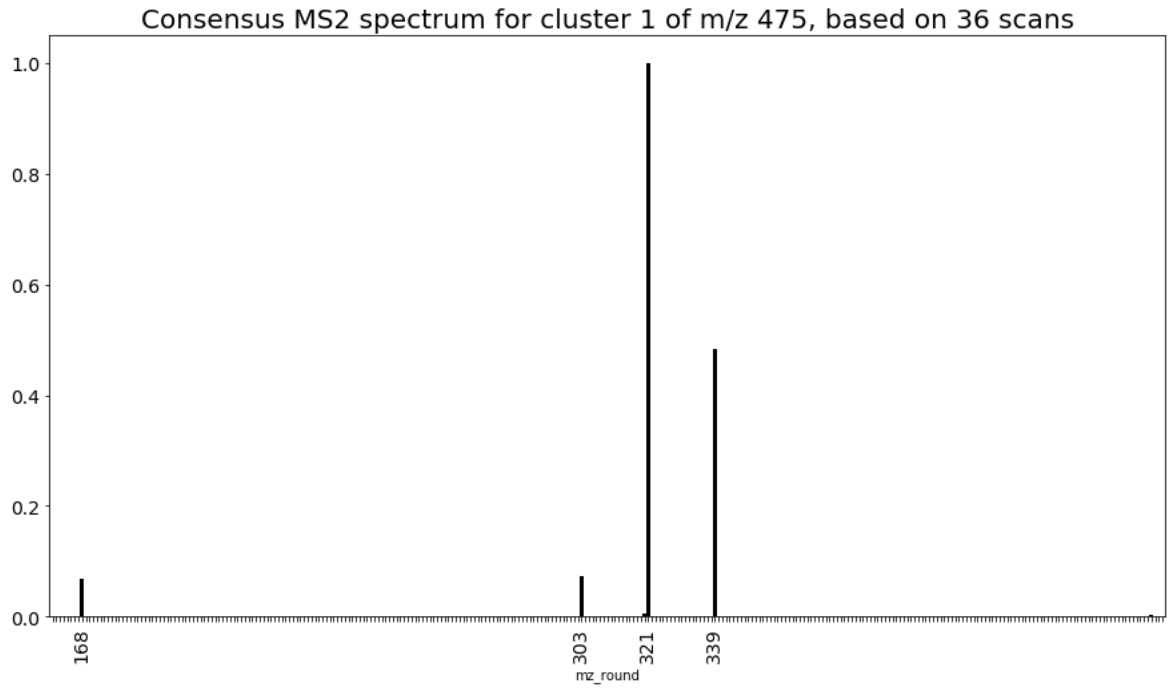


**Figure S23.** Doscadenamide I (**9**) consensus $MS^2$ spectrum

Consensus $MS^2$ spectrum representing a cluster of 36 scans for precursor mass *m*/*z* 475, representing the fragmentation spectrum of the proposed analog doscadenamide I (**9**).

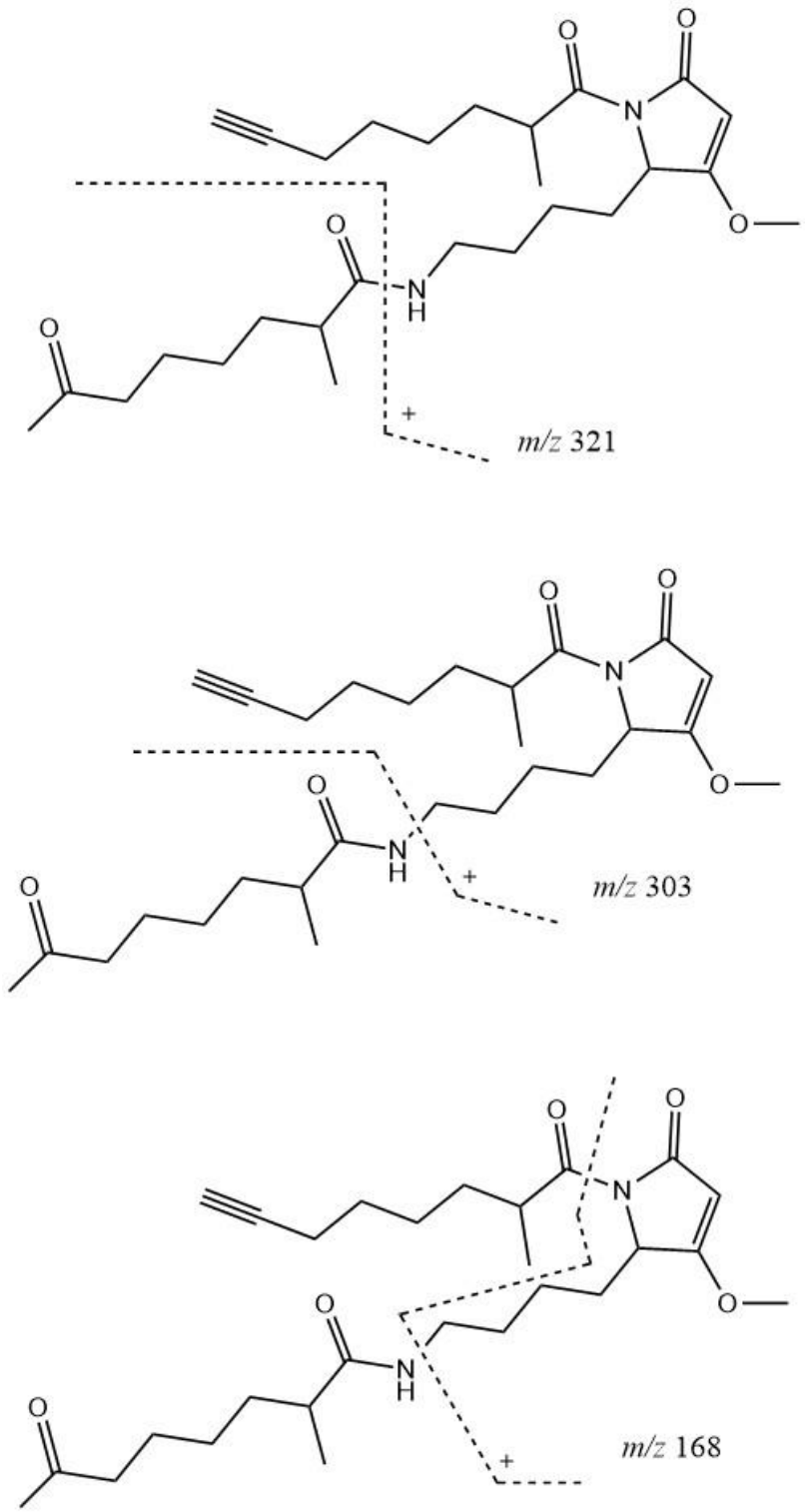


206

207 **Figure S24.** Doscadenamide I (**9**) proposed fragmentation

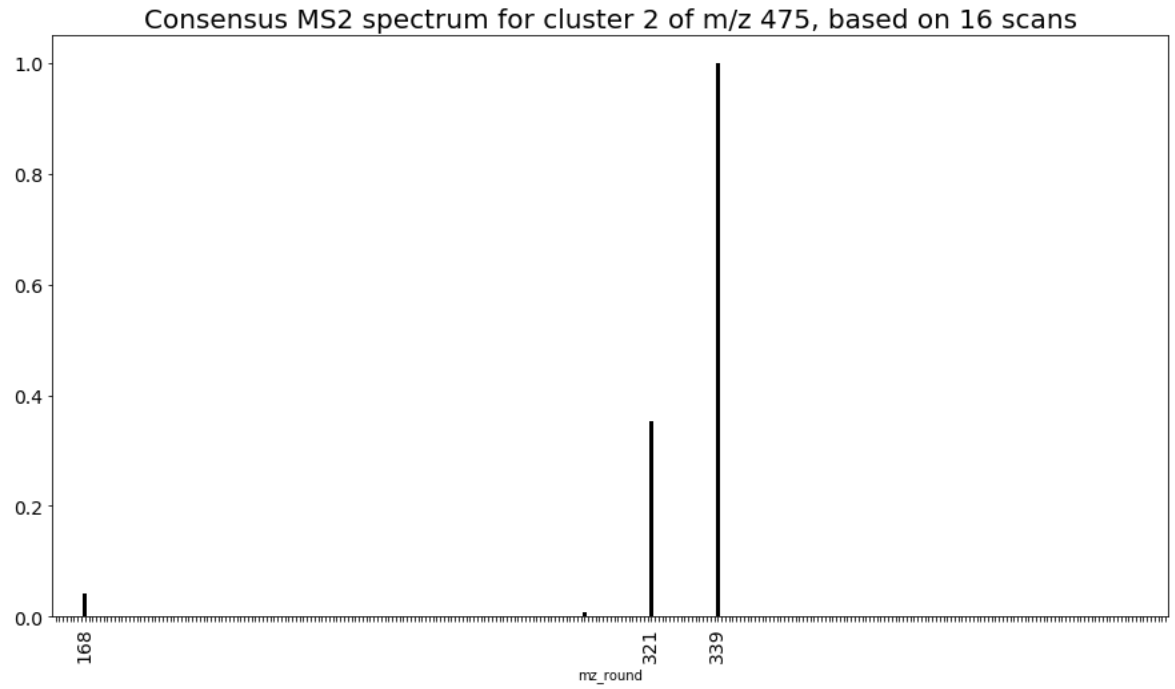


208

209 **Figure S25.** Doscadenamide J (**10**) consensus $MS^2$ spectrum

210 Consensus $MS^2$ spectrum representing a cluster of 16 scans for precursor mass *m*/*z* 475, representing the
211 fragmentation spectrum of the proposed analog doscadenamide J (**10**).

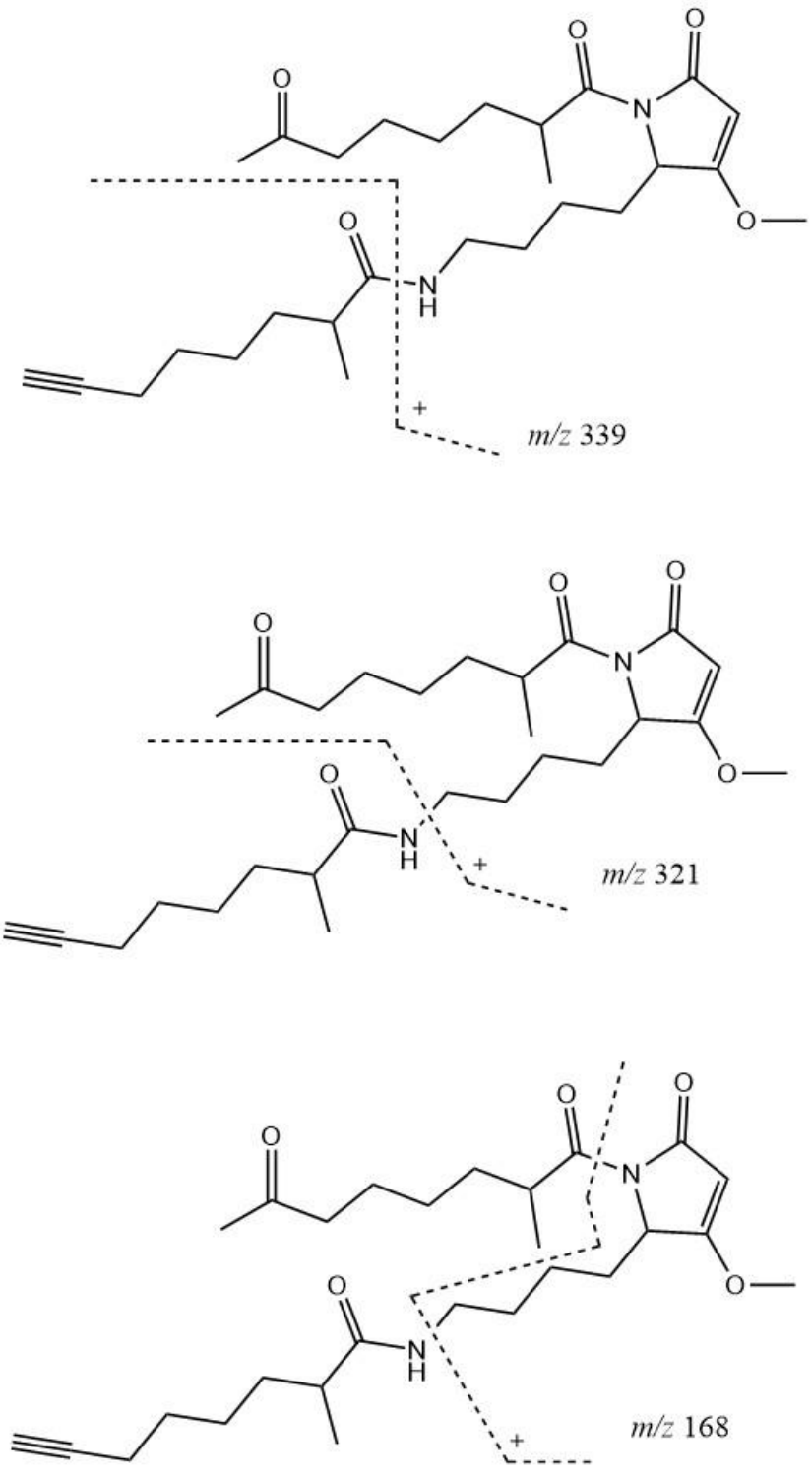


212

213 **Figure S26.** Doscadenamide J (**10**) proposed fragmentation

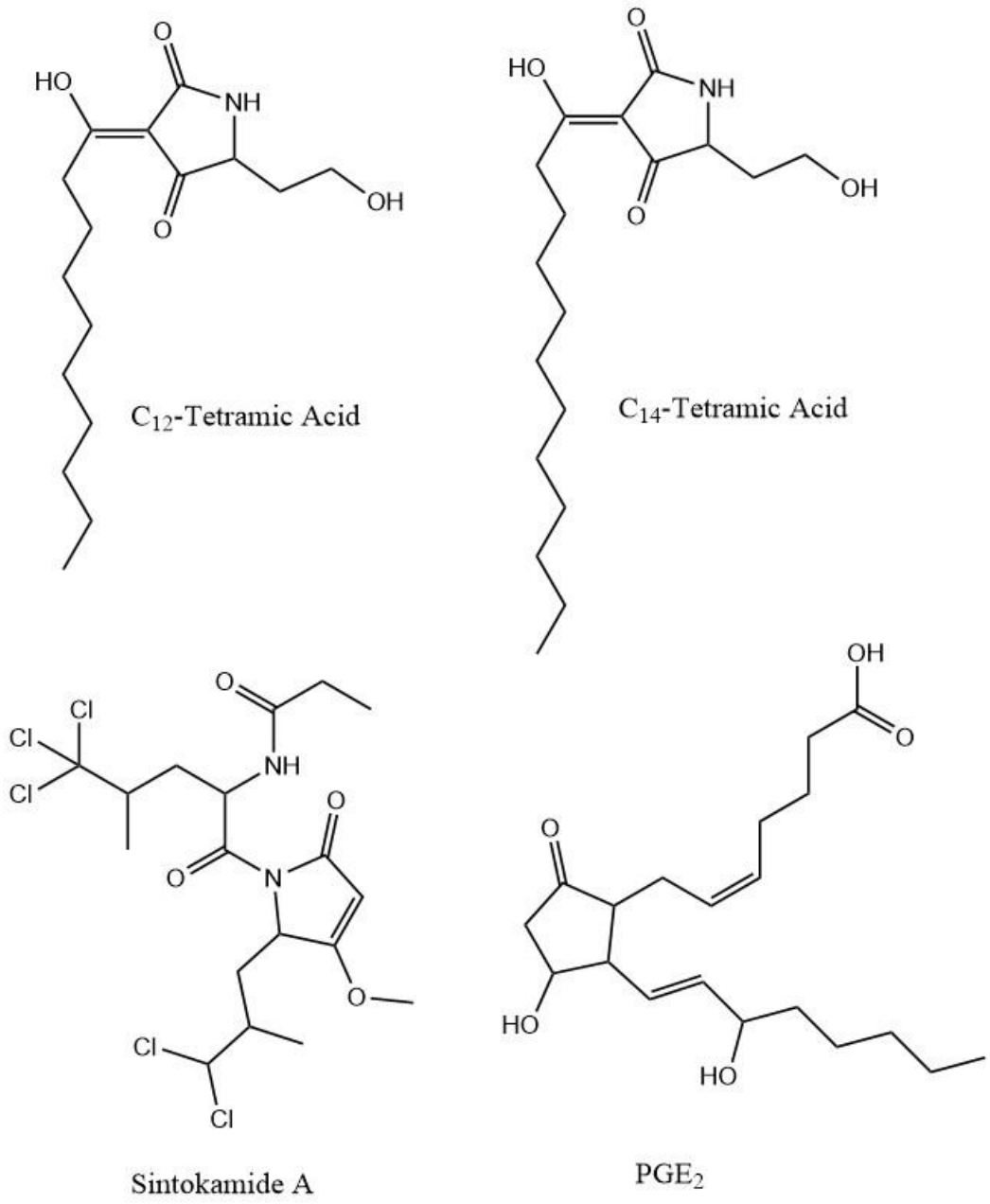


214

215 **Figure S27.** Representative structures from compound families similar to the doscadenamides

216

217

218

219

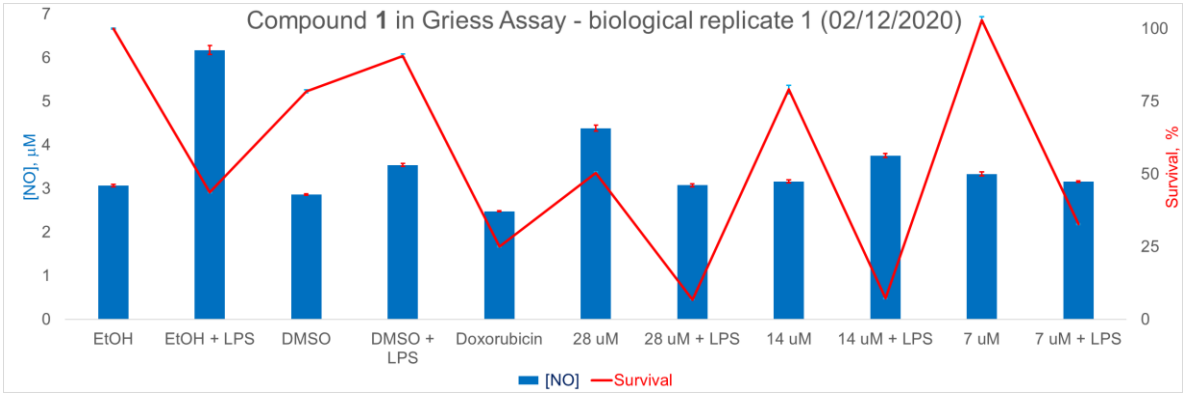


**Figure S28.** Results of compound **1** in Griess assay – biological replicate 1
Reagents were applied at the following concentrations: EtOH (1.5%), LPS (0.5 µg/mL), DMSO (1.0%), and doxorubicin (3.3 µg/mL). One-way ANOVA applied to the survival data indicated statistically significant differences between conditions (p-value < 0.01). Tukey's method was used to determine significance groups: EtOH (a), EtOH + LPS (b), DMSO (c), DMSO + LPS (ac), doxorubicin (d), 28 µM (b), 28 µM + LPS (e), 14 µM (c), 14 µM + LPS (e), 7 µM (a), 7 µM + LPS (d). This result indicates that when compound **1** is applied with LPS, it has a statistically significant negative impact on cell survival, as compared to compound **1** or LPS applied individually, at all three concentrations tested and in a dose-dependent fashion (e.g. when compound **1** was applied at 28 µM and 14 µM, with LPS, it had a statistically significant more negative impact on cell survival than when it was applied at 7 µM with LPS).

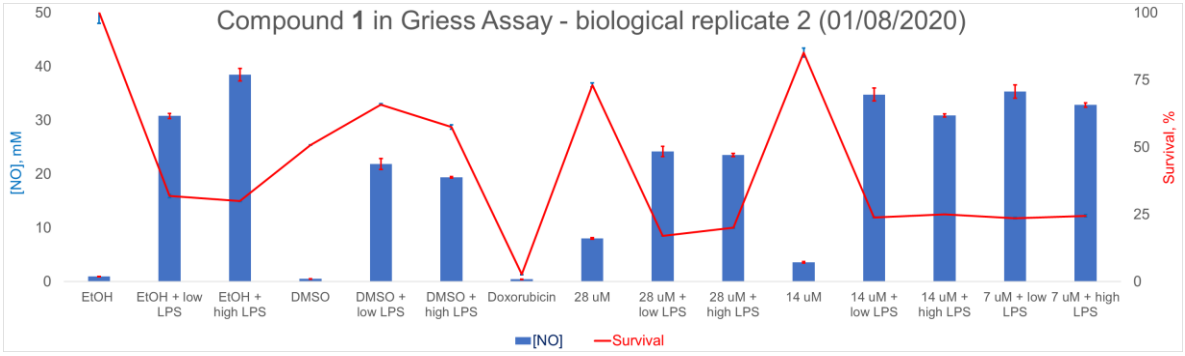


**Figure S29.** Results of compound **1** in Griess assay – biological replicate 2

Reagents were applied at the following concentrations: EtOH (1.0%), low LPS (0.5 µg/mL), high LPS (1.5 µg/mL), DMSO (1.0%), and doxorubicin (3.3 µg/mL). One-way ANOVA applied to the survival data indicated statistically significant differences between conditions (p-value < 0.01). Tukey's method was used to determine significance groups: EtOH (a), EtOH + low LPS (b), EtOH + high LPS (bc), DMSO (d), DMSO + low LPS (e), DMSO + high LPS (de), doxorubicin (f), 28 µM (eg), 28 µM + low LPS (c), 28 µM + high LPS (bc), 14 µM (g), 14 µM + low LPS (bc), 14 µM + high LPS (bc), 7 µM + low LPS (bc), 7 µM + high LPS (bc). No statistically significant difference was found between LPS conditions and compound **1** plus LPS conditions. However, the results still reveal a trend towards compound **1** synergistic cytotoxicity when applied with 0.5 µg/mL LPS, producing an average survival percentage of 17.1, 23.9 and 23.7% at 28, 14 and 7 µM, respectively. In comparison, 0.5 µg/mL LPS applied with EtOH resulted in an average survival of 31.8%.

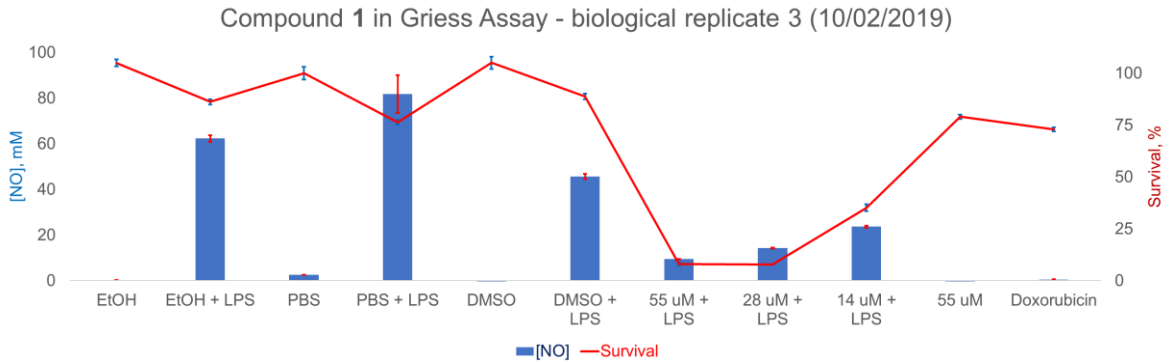


**Figure S30.** Results of compound **1** in Griess assay – biological replicate 3
Reagents were applied at the following concentrations: EtOH (1.0%), LPS (1.5 μg/mL), DMSO (1.0%), and doxorubicin (3.3 μg/mL). Additional control conditions were included in this assay run; phosphate-buffered saline (PBS) with and without LPS was tested. One-way ANOVA applied to the survival data indicated statistically significant differences between conditions (p-value < 0.01). Tukey's method was used to determine significance groups: EtOH (a), EtOH + LPS (ab), PBS (ab), PBS + LPS (ab), DMSO (a), DMSO + LPS (ab), 55 μM + LPS (c), 28 μM + LPS (c), 14 μM + LPS (b), 55 μM (ab), doxorubicin (b). This result illustrates the dose-dependent cytotoxicity of compound **1** when applied with LPS. Statistically significant negative impacts on cell survival were observed when compound **1** was applied with LPS at concentrations of 55 μM and 28 μM, as compared to LPS applied with negative control (EtOH or PBS) and compound **1** applied at 55 μM without LPS.

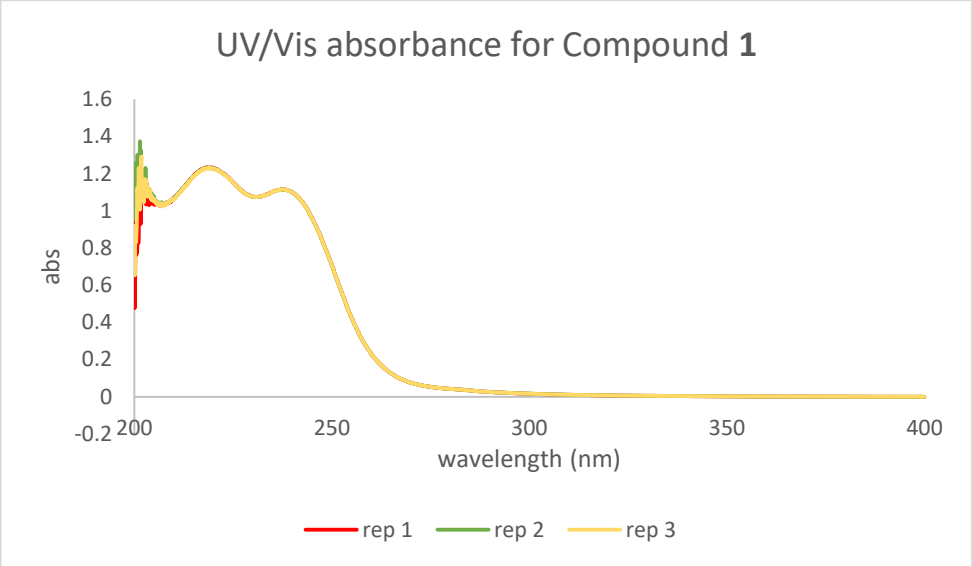


**Figure S31.** UV/Vis absorbance spectrum (200-400 nm) for compound **1**

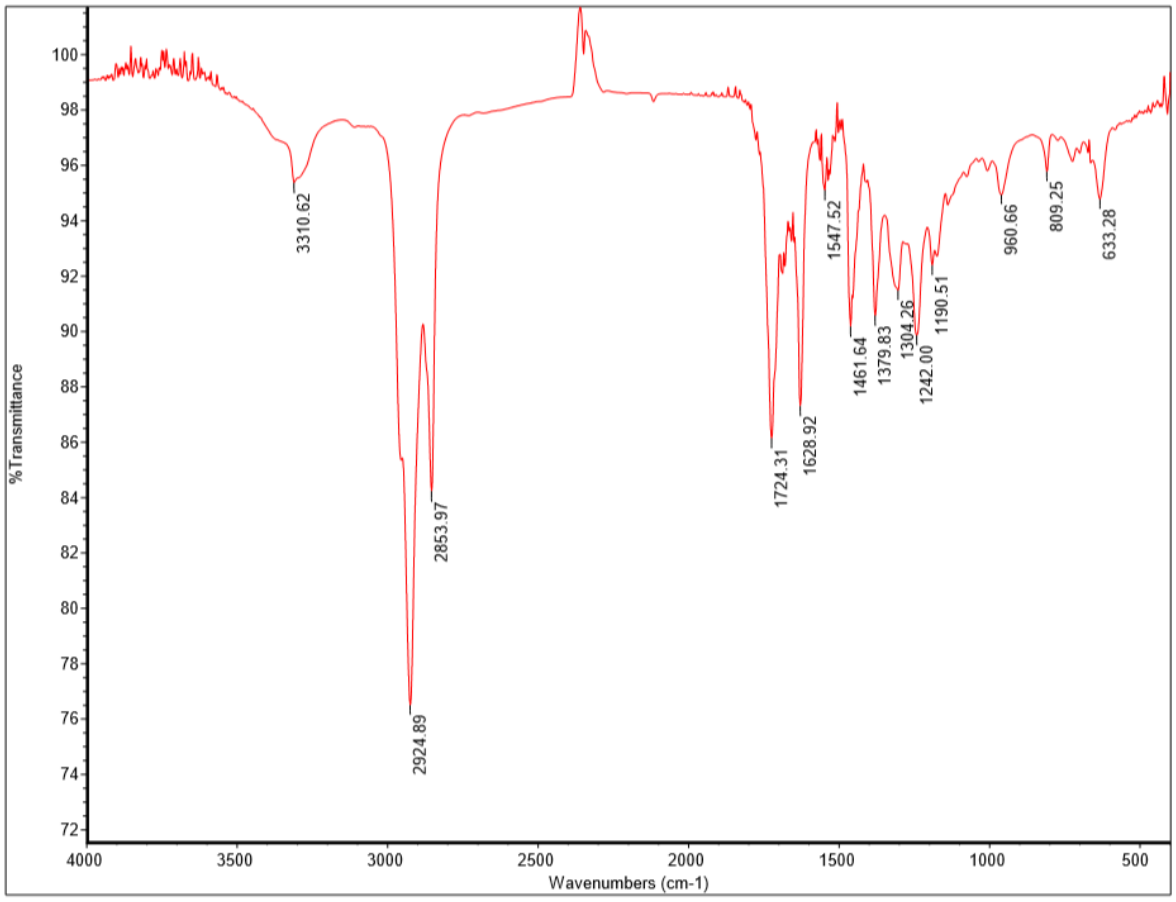


**Figure S32.** IR spectrum for compound **1**

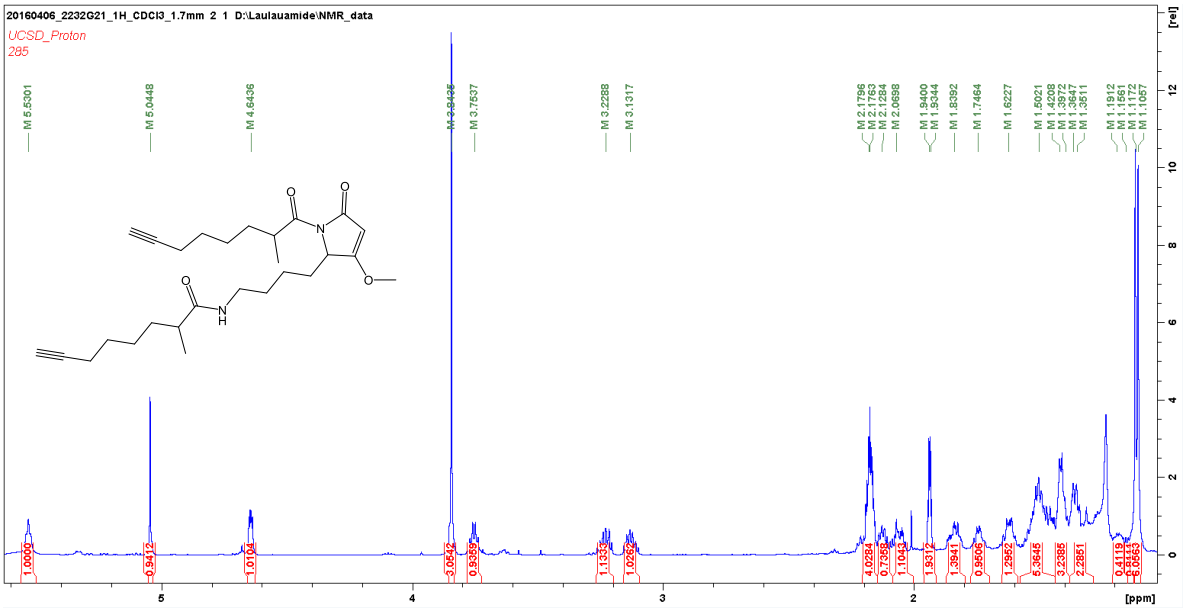


**Figure S33.** $^{1}$H NMR spectrum for compound **1**

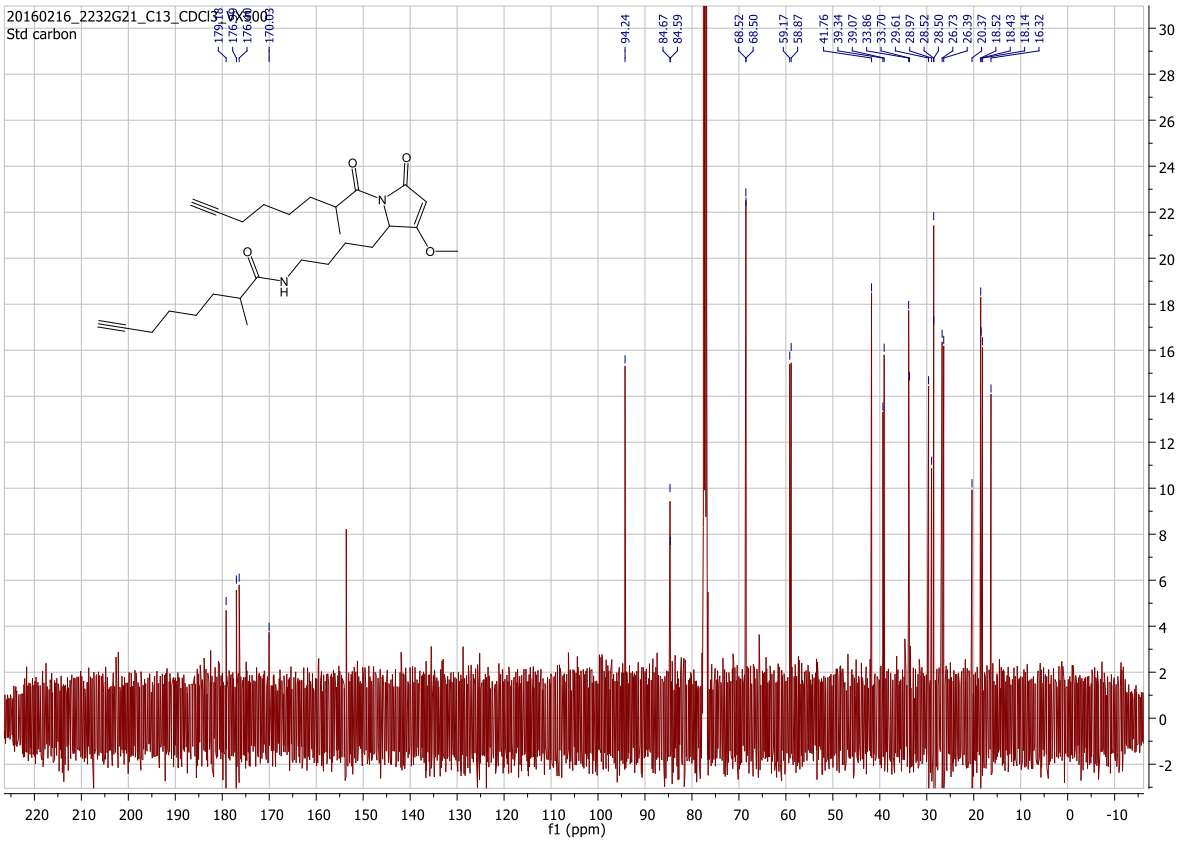


**Figure S34.** $^{13}$C NMR spectrum for compound **1**

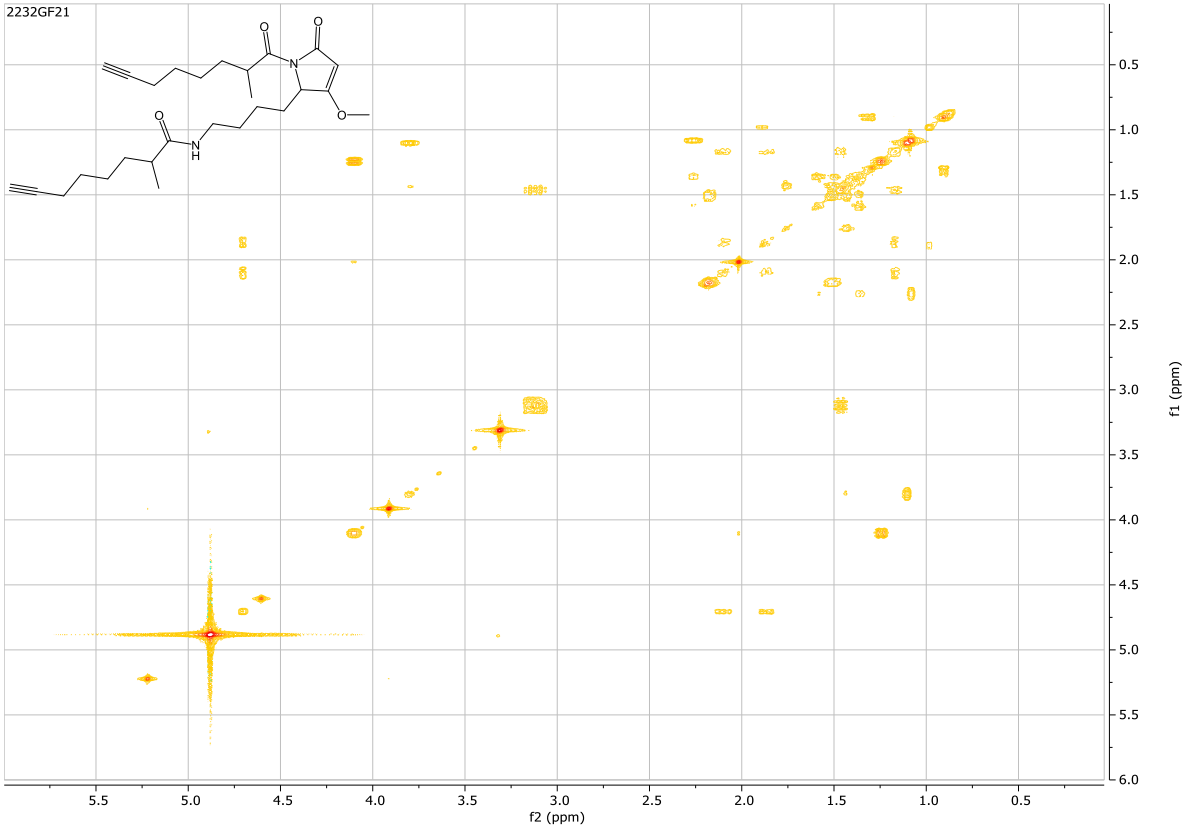


**Figure S35.** $^{1}$H-$^{1}$H COSY spectrum for compound **1**

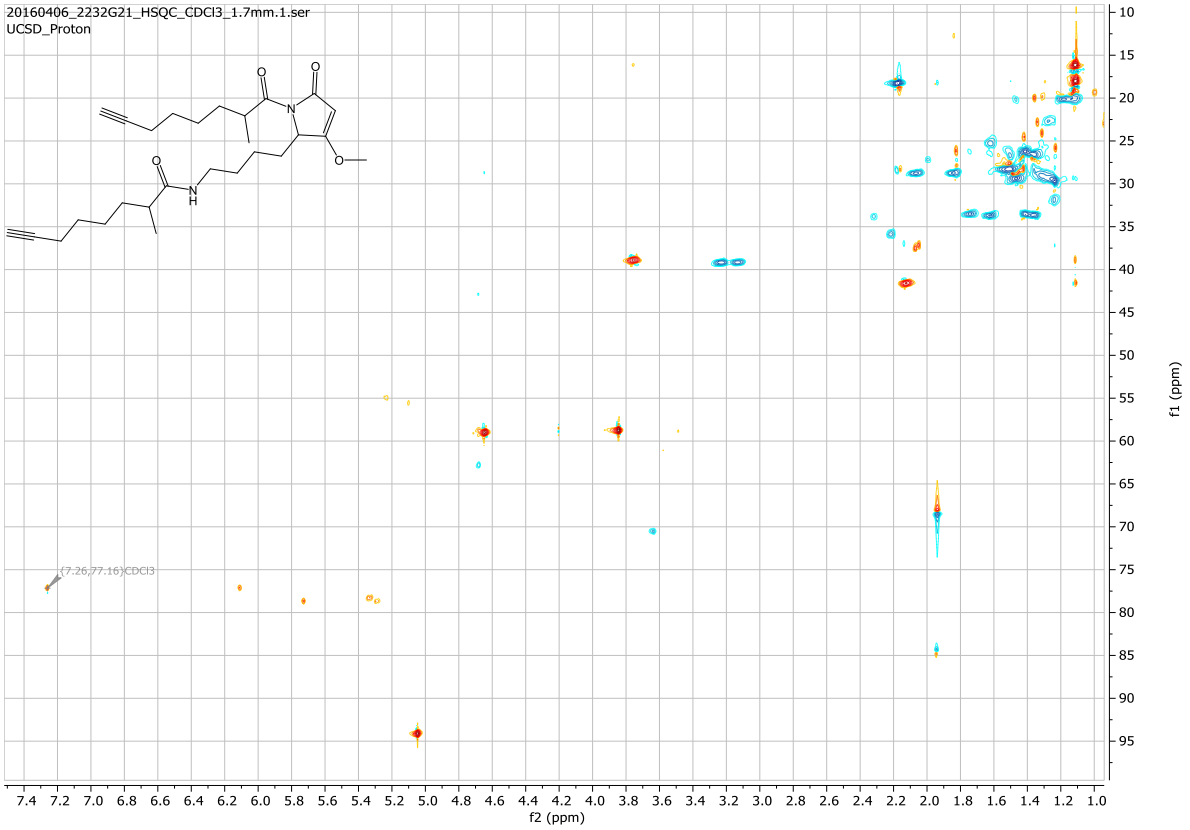


**Figure S36.** $^{1}$H-$^{13}$C HSQC spectrum for compound **1**

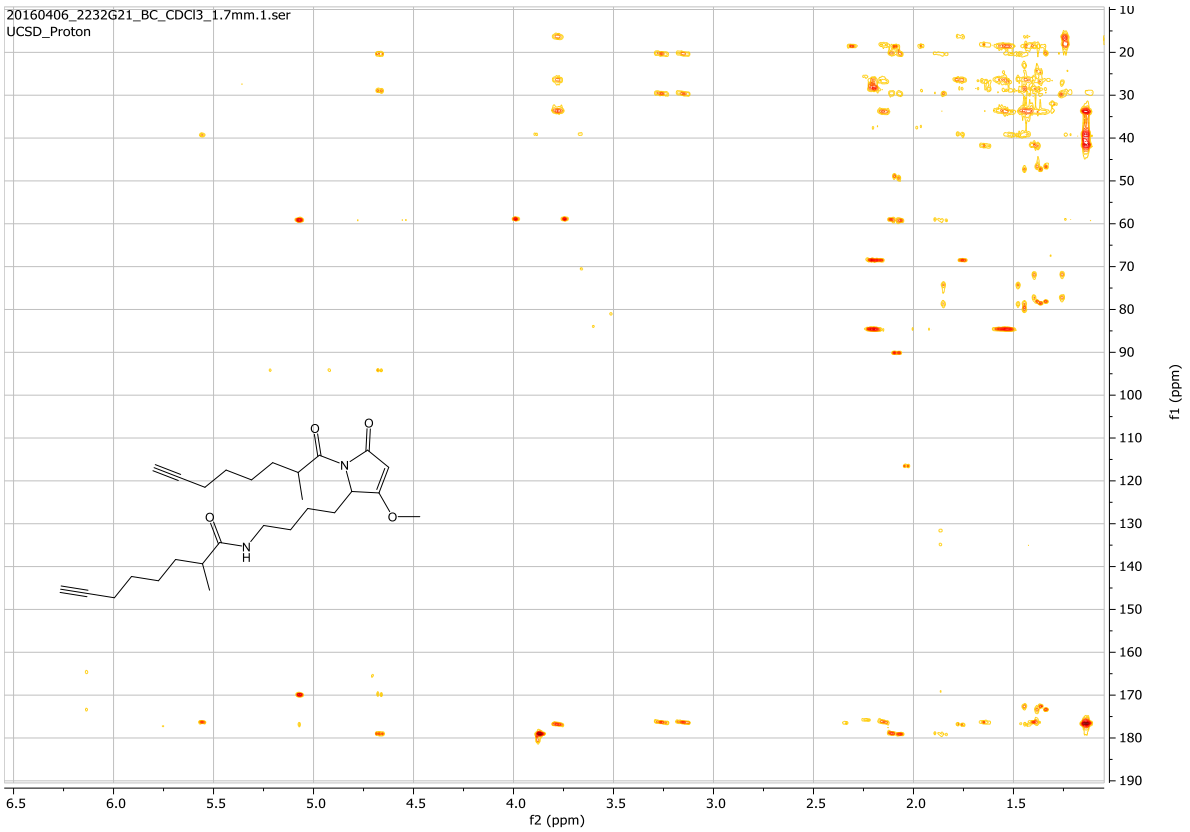


275

276 **Figure S37.** $^{1}H$-$^{13}C$ HMBC spectrum for compound **1**

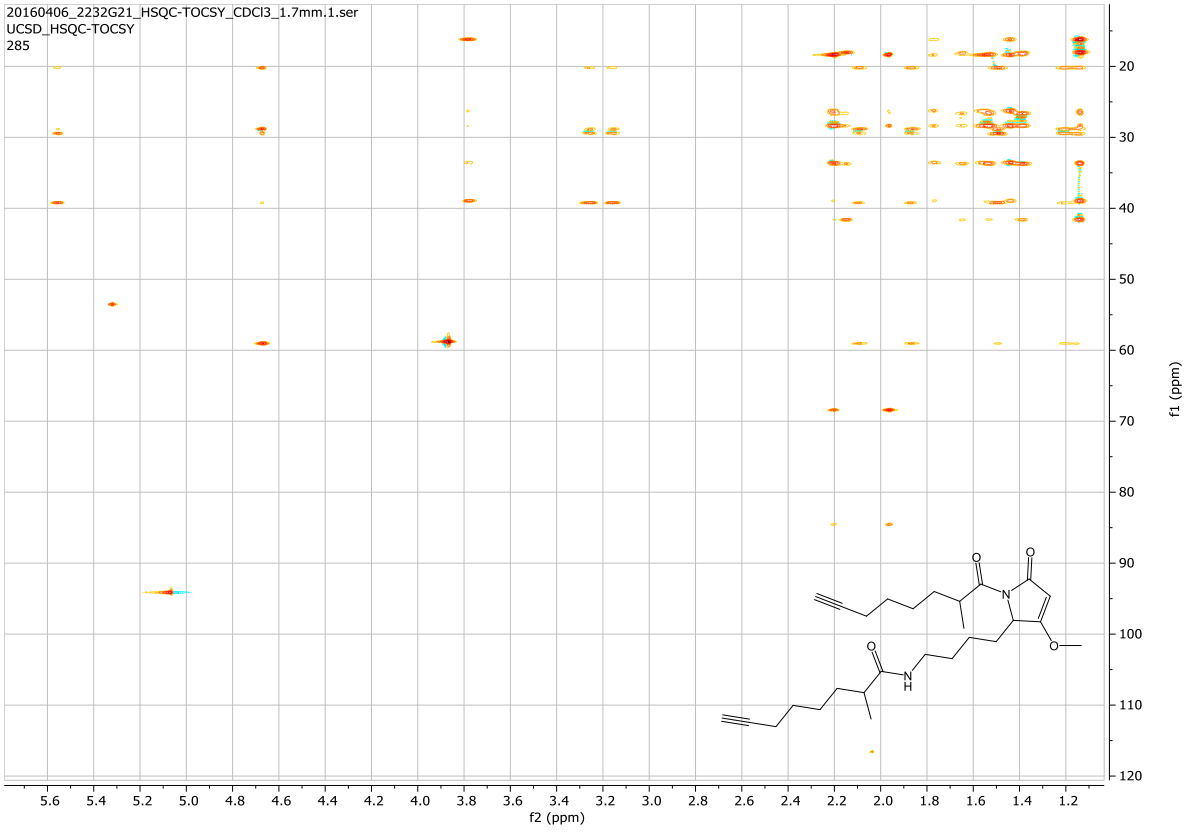


277

278 **Figure S38.** $^{1}H$-$^{13}C$ HSQC-TOCSY spectrum for compound **1**

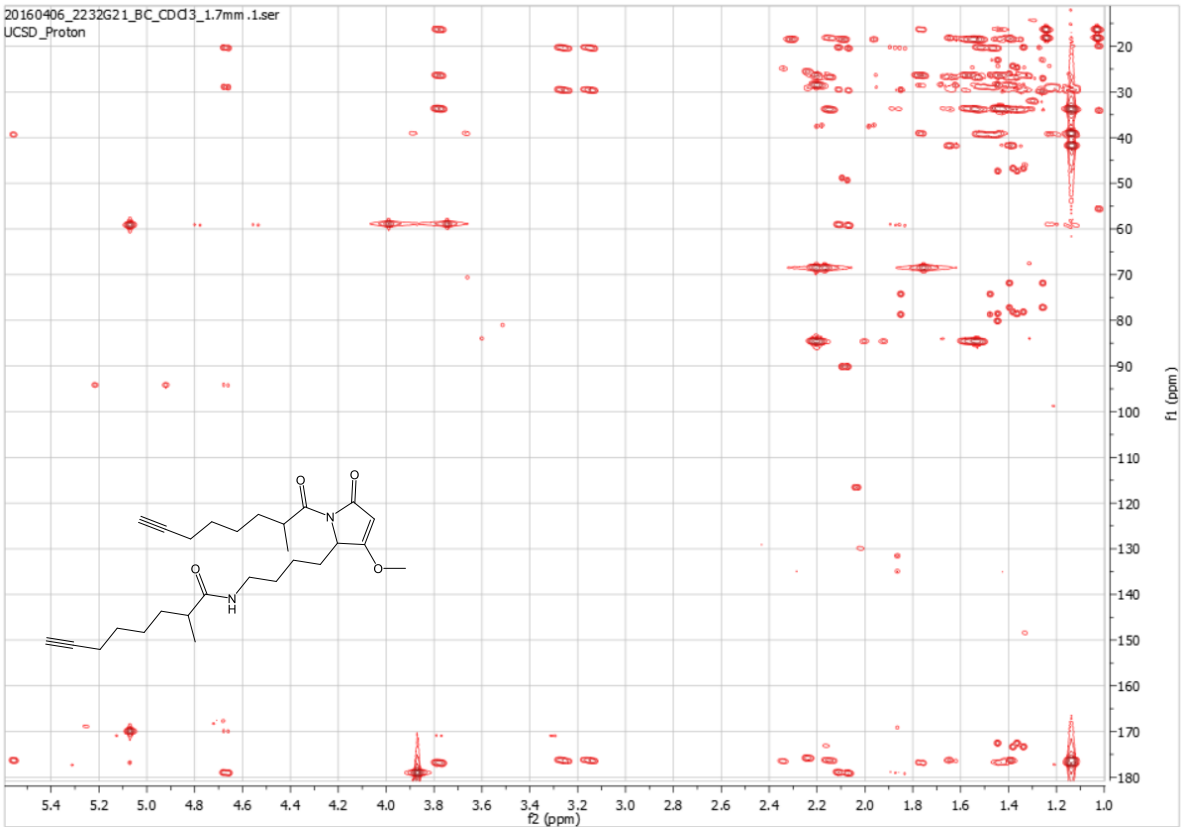


**Figure S39.** $^{1}H$-$^{13}C$ Long-range HSQMBC spectrum for compound **1**

296 **Table S1**. Known compounds isolated from *M. bouillonii*

| Name | Monoisotopic Mass | Protenated Peak | Sodiated Peak | Location of initial isolation | Reference | Notes |
|---|---|---|---|---|---|---|
| **15-norlyngbyapeptin A** | 683.3716 | 684.3786 | 706.3608 | Palau, Guam | [11] | 1 |
| **18E-lyngbyaloside C** | 648.2509 | 649.2579 | 671.2401 | Guam | [12] | |
| **18Z-lyngbyaloside C** | 648.2509 | 649.2579 | 671.2401 | Guam | [12] | |
| **27-deoxylyngbyabellin A** | 674.1766 | 675.1836 | 697.1658 | Guam | [12] | |
| **2-epi-lyngbyaloside** | 660.2509 | 661.2579 | 683.2401 | Guam | [12] | |
| **7-epilyngbyabellin L** | 544.1105 | 545.1175 | 567.0997 | Palmyra Atoll | [13] | |
| **alotamide A** | 587.3393 | 588.3463 | 610.3285 | Papua New Guinea | [14] | |
| **apramide A** | 976.5819 | 977.5889 | 999.5711 | Guam | [15] | |
| **apramide B** | 962.5663 | 963.5733 | 985.5555 | Guam | [15] | |
| **apramide C** | 978.5976 | 979.6046 | 1001.5868 | Guam | [15] | |
| **apramide D** | 1002.5976 | 1003.6046 | 1025.5868 | Guam | [15] | |
| **apramide E** | 988.5819 | 989.5889 | 1011.5711 | Guam | [15] | |
| **apramide F** | 1004.6132 | 1005.6202 | 1027.6024 | Guam | [15] | |
| **apramide G** | 827.5343 | 828.5413 | 850.5235 | Guam | [15] | |
| **apratoxin A** | 839.4866 | 840.4936 | 862.4758 | Guam | [16] | 2 |
| **apratoxin A sulfoxide** | 855.4816 | 856.4886 | 878.4708 | Red Sea | [17] | 3 |
| **apratoxin B** | 825.471 | 826.4780 | 848.4602 | Guam | [18] | 4 |
| **apratoxin C** | 825.471 | 826.4780 | 848.4602 | Palau | [18] | 4 |
| **apratoxin D** | 882.5415 | 883.5485 | 905.5307 | Papua New Guinea | [19] | 5 |
| **apratoxin E** | 795.4604 | 796.4674 | 818.4496 | Guam | [20] | |
| **apratoxin F** | 827.4866 | 828.4936 | 850.4758 | Palmyra Atoll | [21] | |
| **apratoxin G** | 813.471 | 814.4780 | 836.4602 | Palmyra Atoll | [21] | |
| **apratoxin H** | 853.5023 | 854.5093 | 876.4915 | Red Sea | [17] | 3 |
| **apratyramide** | 804.4309 | 805.4379 | 827.4201 | Guam | [22] | |
| **bouillonamide** | 817.49896 | 818.5060 | 840.4882 | Papua New Guinea | [23] | |
| **bouillomide A (lyngbyastatin 9)** | 960.4956 | 961.5026 | 983.4848 | Guam | [24] | |
| **bouillomide B (lyngbyastatin 10)** | 1038.4062 | 1039.4132 | 1061.3954 | Guam | [24] | |
| **columbamide A** | 465.2413 | 466.2483 | 488.2305 | Papua New Guinea | [25] | |
| **columbamide B** | 499.2023 | 500.2093 | 522.1915 | Papua New Guinea | [25] | |
| **columbamide C** | 423.2307 | 424.2377 | 446.2199 | Papua New Guinea | [25] | |
| **columbamide D** | 451.262 | 452.2690 | 474.2512 | Malaysia | [26] | |
| **columbamide E** | 485.223 | 486.2300 | 508.2122 | Malaysia | [26] | |
| **columbamide F** | 493.2726 | 494.2796 | 516.2618 | Malaysia | [27] | |
| **columbamide G** | 527.2336 | 528.2406 | 550.2228 | Malaysia | [27] | |
| **columbamide H** | 417.301 | 418.3080 | 440.2902 | Malaysia | [27] | |
| **cyanolide A** | 832.482 | 833.4890 | 855.4712 | Papua New Guinea | [28] | |
| **doscadenamide A** | 456.2988 | 457.3058 | 479.2880 | Guam | [29] | |
| **kakeromamide A** | 790.4088 | 791.4158 | 813.3980 | Japan | [30] | |
| **kakeromamide B** | 790.4088 | 791.4158 | 813.3980 | Fiji | [31] | 6 |
| **kanamienamide** | 492.3563 | 493.3633 | 515.3455 | Japan | [32] | |
| **laingolide** | 351.2773 | 352.2843 | 374.2665 | Papua New Guinea | [33] | |
| **laingolide A** | 337.2617 | 338.2687 | 360.2509 | Papua New Guinea | [34] | |
| **laingolide B** | 369.2071 | 370.2141 | 392.1963 | Guam | [12] | |
| **lyngbouilloside** | 584.356 | 585.3630 | 607.3452 | Papua New Guinea | [35] | |
| **lyngbyabellin A** | 690.1715 | 691.1785 | 713.1607 | Guam | [36] | 2 |
| **lyngbyabellin B** | 678.1715 | 679.1785 | 701.1607 | Guam | [37] | 2 |
| **lyngbyabellin C** | 608.082 | 609.0890 | 631.0712 | Palau | [38] | 1 |
| **lyngbyabellin D** | 895.2553 | 896.2623 | 918.2445 | Palau, Guam | [11] | 1 |
| **lyngbyabellin J** | 863.2291 | 864.2361 | 886.2183 | Guam | [12] | |
| **lyngbyabellin K** | 578.0715 | 579.0785 | 601.0607 | Palmyra Atoll | [13] | |
| **lyngbyabellin L** | 544.1105 | 545.1175 | 567.0997 | Palmyra Atoll | [13] | |
| **lyngbyabellin M** | 624.1133 | 625.1203 | 647.1025 | Palmyra Atoll | [13] | |
| **lyngbyabellin N** | 904.292 | 905.2990 | 927.2812 | Palmyra Atoll | [13] | |
| **lyngbyaloside** | 660.2509 | 661.2579 | 683.2401 | Papua New Guinea | [39] | |
| **lyngbyaloside B** | 648.2509 | 649.2579 | 671.2401 | Palau | [40] | 1 |
| **lyngbyapeptin A** | 697.3873 | 698.3943 | 720.3765 | Papua New Guinea | [41] | |
| **lyngbyapeptin B** | 721.3509 | 722.3579 | 744.3401 | Palau | [38] | 1 |
| **lyngbyapeptin C** | 735.3665 | 736.3735 | 758.3557 | Palau | [38] | 1 |
| **lyngbyapeptin D** | 683.3716 | 684.3786 | 706.3608 | Guam | [12] | |

| | | | | | | |
|---|---|---|---|---|---|---|
| **lyngbyastatin 2** | 1058.6878 | 1059.6948 | 1081.6770 | Guam | [42] | 2 |
| **mandangolide** | 377.561 | 378.5680 | 400.5502 | Papua New Guinea | [34] | |
| **mooreamide A** | 389.293 | 390.3000 | 412.2822 | Papua New Guinea | [43] | |
| **norlyngbyastatin 2** | 1044.6722 | 1045.6792 | 1067.6614 | Guam | [42] | 2 |
| **palau'imide** | 428.2675 | 429.2745 | 451.2567 | Palau | [38] | 1 |
| **ulongamide A** | 627.309 | 628.3160 | 650.2982 | Palau | [44] | 1 |
| **ulongamide B** | 643.3039 | 644.3109 | 666.2931 | Palau | [44] | 1 |
| **ulongamide C** | 691.3039 | 692.3109 | 714.2931 | Palau | [44] | 1 |
| **ulongamide D** | 671.3352 | 672.3422 | 694.3244 | Palau | [44] | 1 |
| **ulongamide E** | 685.3509 | 686.3579 | 708.3401 | Palau | [44] | 1 |
| **ulongamide F** | 607.3403 | 608.3473 | 630.3295 | Palau | [44] | 1 |

[1]Reported as *Lyngbya sp.*; cited in subsequent publications as *M. bouillonii*

[2]Reported as *Lyngbya majuscula*; cited in subsequent publications as *M. bouillonii*

[3]Reported as *Moorea producens*; 16S classification inconclusive; chemistry associated with *M. bouillonii*

[4]Reported as *Lyngbya sp.*; but cited in subsequent publications as *M. bouillonii* and reported to grow with *Alpheus frontalis*

[5]Reported as *Lyngbya majuscula* and *Lyngbya sordid*; 16S classification inconclusive; chemistry associated with *M. bouillonii*

[6]Reported as *Moorea producens*; manuscript includes a photo of woven *M. bouillonii*; 16S classification inconclusive; compound isolated along with known compounds previously isolated from *M. bouillonii*

**Table S2.** Average relative abundances and feature selection scores for top 10 Saipan MS[1] features

| *m/z* | relative rt | F-value[1] | p-value[1] | American Samoa[2] | China[2] | Guam[2] | India[2] | PNG[2] | Saipan[2] |
|---|---|---|---|---|---|---|---|---|---|
| 721.10 | 0.6065 | 0.869 | 0.5371 | 0.045 | 0.025 | 0 | 0 | 0.007 | 0.210 |
| **457.05**[3] | **0.4852** | **17.402** | **0.0002** | **0.012** | **0.023** | **0.006** | **0** | **0.005** | **0.176** |
| 1368.03 | 0.5654 | 5.049 | 0.0176 | 0.011 | 0.035 | 0.014 | 0.008 | 0.005 | 0.175 |
| 609.10 | 0.6263 | 1.229 | 0.3704 | 0.049 | 0.028 | 0.050 | 0.126 | 0.010 | 0.172 |
| 535.10 | 0.6177 | 2.073 | 0.1613 | 0.065 | 0.034 | 0.214 | 0.005 | 0 | 0.158 |
| 1367.06 | 0.5626 | 2.314 | 0.1296 | 0.008 | 0.027 | 0.030 | 0.069 | 0 | 0.136 |
| 459.06 | 0.5141 | 31.678 | < 0.0001 | 0 | 0.024 | 0.006 | 0.005 | 0 | 0.112 |
| 536.10 | 0.6270 | 3.205 | 0.0617 | 0.094 | 0.014 | 0.034 | 0.006 | 0.006 | 0.102 |
| 1687.01 | 0.4942 | 1.086 | 0.4296 | 0.005 | 0.008 | 0 | 0.019 | 0.005 | 0.100 |
| 722.04 | 0.5938 | 0.703 | 0.6356 | 0.035 | 0.010 | 0.015 | 0.008 | 0.004 | 0.096 |

[1]F-values and p-values are generated in ORCA using the scikit learn (https://scikit-learn.org/stable/) implementation of univariate feature selection. These scores should be interpreted cautiously, as the dataset does not meet the assumptions necessary for univariate features selection, but can still help in generating hypotheses about which features are driving differences between samples collected from different geographical regions.

[2]Average of the unit vector normalized integrated feature values for all samples from the geographical region.

[3]Compound **1** was detected in high abundance in samples from Saipan, ranking as the second most abundant MS[1] feature, while not being detected or being detected at very low levels in other samples.

329 **Table S3.** Putative identifications for the top 30 MS[1] features in the *M. bouillonii* crude extract dataset

| | m/z | relative rt | max transformed integral | putative ids | difference |
|---|---|---|---|---|---|
| 1 | 815.10 | 0.6383 | 0.857928 | ['apratoxin G [M+H]+'] | [0.62] |
| 2 | 814.06 | 0.5968 | 0.765564 | ['apratoxin G [M+H]+', 'kakeromamide A [M+Na]+', 'kakeromamide B [M+Na]+'] | [0.42, 0.66, 0.66] |
| 3 | 721.10 | 0.6065 | 0.572637 | ['lyngbyapeptin A [M+Na]+'] | [0.73] |
| 4 | 840.07 | 0.6350 | 0.510516 | ['apratoxin A [M+H]+', 'bouilllonamide [M+Na]+'] | [0.43, 0.42] |
| 5 | 862.08 | 0.5894 | 0.508103 | ['apratoxin A [M+Na]+'] | [0.39] |
| 6 | 623.10 | 0.6501 | 0.440651 | ['None'] | [0] |
| 7 | 611.09 | 0.5845 | 0.427792 | ['alotamide A [M+Na]+'] | [0.77] |
| 8 | 678.10 | 0.5988 | 0.386879 | ['None'] | [0] |
| 9 | 535.10 | 0.6177 | 0.382478 | ['None'] | [0] |
| 10 | 609.10 | 0.6263 | 0.369167 | ['lyngbyabellin C [M+H]+', 'ulongamide F [M+H]+'] | [0.01, 0.75] |
| 11 | 378.06 | 0.5832 | 0.35347 | ['mandangolide [M+H]+'] | [0.5] |
| 12 | 625.11 | 0.6320 | 0.334295 | ['lyngbyabellin M [M+H]+'] | [0.01] |
| 13 | 793.11 | 0.6292 | 0.326725 | ['None'] | [0] |
| 14 | 827.10 | 0.6185 | 0.312621 | ['apratoxin B [M+H]+', 'apratoxin C [M+H]+', 'apratyramide [M+Na]+'] | [0.62, 0.62, 0.32] |
| 15 | 744.09 | 0.6160 | 0.31144 | ['lyngbyapeptin B [M+Na]+'] | [0.25] |
| 16 | 836.08 | 0.6534 | 0.286632 | ['apratoxin G [M+Na]+'] | [0.38] |
| 17 | 1368.02 | 0.5654 | 0.280465 | ['None'] | [0] |
| 18 | 639.08 | 0.6220 | 0.279184 | ['None'] | [0] |
| 19 | 581.10 | 0.6134 | 0.277933 | ['None'] | [0] |
| 20 | 632.10 | 0.6188 | 0.274745 | ['None'] | [0] |
| 21 | 722.04 | 0.5938 | 0.266215 | ['lyngbyapeptin B [M+H]+'] | [0.32] |
| 22 | 886.05 | 0.6135 | 0.258829 | ['lyngbyabellin J [M+Na]+'] | [0.17] |
| 23 | 841.13 | 0.6118 | 0.24873 | ['apratoxin A [M+H]+', 'bouilllonamide [M+Na]+'] | [0.63, 0.64] |
| 24 | 651.11 | 0.6804 | 0.246204 | ['ulongamide A [M+Na]+'] | [0.81] |
| 25 | 1687.01 | 0.4942 | 0.245016 | ['None'] | [0] |
| **26** | **457.05** | **0.4852** | **0.242068** | **['None'][1]** | **[0]** |
| 27 | 1367.06 | 0.5627 | 0.22625 | ['None'] | [0] |
| 28 | 816.09 | 0.6681 | 0.224017 | ['None'] | [0] |
| 29 | 494.07 | 0.6387 | 0.21453 | ['columbamide F [M+H]+', 'kanamienamide [M+H]+'] | [0.21, 0.71] |
| 30 | 863.09 | 0.6430 | 0.209889 | ['apratoxin A [M+Na]+'] | [0.61] |

330 [1]No putative identifications were assigned to compound **1**, suggesting it to be a new natural product.

331 **Table S4.** *In silico* antibiotic screening results for the doscadenamides and tetramic acids

| compound name | SMILES | score[1] |
|---|---|---|
| doscadenamides A | COC1=CC(N(C(C(C)CCCCC#C)=O)C1CCCCNC(C(C)CCCCC#C)=O)=O | 0.031352468 |
| doscadenamides B | COC1=CC(N(C(C(C)CCCCC=C)=O)C1CCCCNC(C(C)CCCCC=C)=O)=O | 0.056482284 |
| doscadenamides C | COC1=CC(N(C(C(C)CCCCC#C)=O)C1CCCCNC(C(C)CCCCC=C)=O)=O | 0.038773874 |
| doscadenamides D | COC1=CC(N(C(C(C)CCCCC=C)=O)C1CCCCNC(C(C)CCCCC#C)=O)=O | 0.038728081 |
| doscadenamides E | COC1=CC(N(C(C(C)CCCCC#C)=O)C1CCCCNC(C(C)CCCCCC)=O)=O | 0.062902918 |
| doscadenamides F | COC1=CC(N(C(C(C)CCCCCC)=O)C1CCCCNC(C(C)CCCCC#C)=O)=O | 0.0636456 |
| doscadenamides G | COC1=CC(N(C(C(C)CCCCC=C)=O)C1CCCCNC(C(C)CCCCCC)=O)=O | 0.091586996 |
| doscadenamides H | COC1=CC(N(C(C(C)CCCCCC)=O)C1CCCCNC(C(C)CCCCC=C)=O)=O | 0.092198204 |
| doscadenamides I | COC1=CC(N(C(C(C)CCCCC#C)=O)C1CCCCNC(C(C)CCCCC(C)=O)=O)=O | 0.049369105 |
| doscadenamides J | COC1=CC(N(C(C(C)CCCCC(C)=O)=O)C1CCCCNC(C(C)CCCCC#C)=O)=O | 0.04936365 |
| $C_{12}$-tetramic acid | O=C(/C1=C(O)/CCCCCCCCC)NC(CCO)C1=O | 0.545725947 |
| $C_{14}$-tetramic acid | O=C(/C1=C(O)/CCCCCCCCCCC)NC(CCO)C1=O | 0.590775286 |

332 [1] Scores represent the probability that the screened compound would inhibit *E. coli* growth at 50 μM [78].

333 **Table S5.** *M. bouillonii* crude extract sample metadata

| filename | alias | extract number | collection code | collection country/territory | collection region | collection site | collection date |
|---|---|---|---|---|---|---|---|
| 20170915_CBN_XSSCB2017_13.mzXML | China_13 | - | XSSCB2017_13 | China/Xisha | Sanshax | 16° 51' 05.52", 112° 20' 56.13" | 5/16/2017 |
| 20170915_CBN_XSSCB2017_24.mzXML | China_24 | - | XSSCB2017_24 | China/Xisha | Sanshax | 16° 51' 05.52", 112° 20' 56.13" | 5/19/2017 |
| 20170915_CBN_XSSCB2017_25.mzXML | China_25 | - | XSSCB2017_25 | China/Xisha | Sanshax | 16° 51' 05.52", 112° 20' 56.13" | 5/19/2017 |
| 2019-08-23_CBN_KHI-18-1.mzXML | India_KHI | - | KHT08APR18-3 | India/Lakshadweep | Kavaratti | Heaven's Treat lagoon | 4/8/2018 |
| 2019-08-23_CBN_KP-16-1.mzXML | India_KP | - | KP-16 | India/Lakshadweep | Kavaratti | Paradise Hut lagoon | 2/6/2016 |
| 2019-08-23_CBN_KPL-18-1.mzXML | India_KPL | - | KPL08APR18-1 | India/Lakshadweep | Kavaratti | Paradise Hut lagoon | 4/8/2018 |
| 2019-08-23_CBN_KSP-18-1.mzXML | India_KSP | - | KSP07APR18-1 | India/Lakshadweep | Kavaratti | south of Paradise Hut pier | 4/7/2018 |
| 2200.mzXML | Saipan_00 | 2200 | SPB31JAN13-1 | Saipan | - | Laulau Bay | 1/31/2013 |
| 2209.mzXML | Saipan_09 | 2209 | SPD29JAN13-6 | Saipan | - | Laulau Bay | 1/29/2013 |
| 2220.mzXML | AmSam_20 | 2220 | ASA12JUL14-1 | American Samoa | - | Afao | 7/12/2014 |
| 2223.mzXML | AmSam_23 | 2223 | ASG15JUL14-1 | American Samoa | - | Fagasa Bay | 7/15/2014 |
| 2232.mzXML | Saipan_32 | 2232 | SPB01FEB13-1 | Saipan | - | Laulau Bay | 2/1/2013 |
| 2246.mzXML | Guam_46 | 2246 | GBB21MAR16-1 | Guam | - | Apra Harbor | 3/21/2016 |
| 2247.mzXML | Guam_47 | 2247 | GGG21MAR16-1 | Guam | - | Apra Harbor | 3/21/2016 |
| Mb.mzXML | PNG_c | - | PNG19MAY05-8 | Papua New Guinea | New Ireland | Pigeon Island | 5/19/2005 |

334

335 **Table S6.** ORCA parameter set for $MS^1$ feature dendrogram

| parameter | value |
|---|---|
| bin_width | 0.5 |
| bin_offset | 0 |
| bins_start | 200 |
| bins_end | 2000 |
| peak_consecutivity | 0 |
| peak_cluster_size_cutoff | 3 |
| min_integral | 100000 |
| rt_setting | 'relative' |
| rrt_tolerance | 0.05 |
| transforms | None |
| metric | 'cosine' |
| method | 'average' |
| color_cutoff | N/A (custom colorization) |

336

337

338 **Table S7.** ORCA parameter set for GNPS $MS^2$ feature presence/absence dendrogram

| parameter | value |
|---|---|
| drop_columns | ['#OTU ID'] |
| drop_rows | [] |
| transpose_buckettable | False |
| transforms | presence_absence = True |
| metric | 'cosine' |
| method | 'average' |
| color_cutoff | N/A (custom colorization) |

339

340 **Table S8.** ORCA parameter set for $MS^1$ feature selection

| parameter | value |
|---|---|
| bin_width | 1 |
| bin_offset | 0 |
| bins_start | 200 |
| bins_end | 2000 |
| peak_consecutivity | 0 |
| peak_cluster_size_cutoff | 3 |
| min_integral | 100000 |
| rt_setting | 'relative' |
| rrt_tolerance | 0.05 |
| transforms | None |
| metric | 'cosine' |
| method | 'average' |
| color_cutoff | N/A (custom colorization) |

341

342

343

344

345

346

347

348

349

350

351

352 **Table S9.** GNPS parameter set for *M. bouillonii* crude extract molecular network

| parameter | value |
|---|---|
| workflow version | 1.2.5 |
| PAIRS_MIN_COSINE | 0.7 |
| ANALOG_SEARCH | 1 |
| tolerance.PM_tolerance | 2.0 |
| tolerance.Ion_tolerance | 0.5 |
| MIN_MATCHED_PEAKS | 2 |
| TOPK | 10 |
| CLUSTER_MIN_SIZE | 1 |
| MAXIMUM_COMPONENT_SIZE | 100 |
| MIN_PEAK_INT | 50 |
| FILTER_STDDEV_PEAK_INT | 0.0 |
| RUN_MSCLUSTER | on |
| FILTER_PRECURSOR_WINDOW | 1 |
| FILTER_LIBRARY | 1 |
| WINDOW_FILTER | 1 |
| SCORE_THRESHOLD | 0.7 |
| MIN_MATCHED_PEAKS_SEARCH | 2 |
| MAX_SHIFT_MASS | 100.0 |

353

354 **Table S10.** GNPS parameter set for *M. bouillonii* crude extract $MS^2$ feature bucket table

| parameter | value |
|---|---|
| workflow version | release_22 |
| PAIRS_MIN_COSINE | 0.7 |
| ANALOG_SEARCH | 1 |
| tolerance.PM_tolerance | 2.0 |
| tolerance.Ion_tolerance | 0.5 |
| MIN_MATCHED_PEAKS | 4 |
| TOPK | 10 |
| CLUSTER_MIN_SIZE | 1 |
| MAXIMUM_COMPONENT_SIZE | 100 |
| MIN_PEAK_INT | 0.0 |
| FILTER_STDDEV_PEAK_INT | 0.0 |
| RUN_MSCLUSTER | on |
| FILTER_PRECURSOR_WINDOW | 1 |
| FILTER_LIBRARY | 1 |
| WINDOW_FILTER | 1 |
| SCORE_THRESHOLD | 0.7 |
| MIN_MATCHED_PEAKS_SEARCH | 4 |
| MAX_SHIFT_MASS | 100.0 |

355 **Table S11.** GNPS parameter set for Saipan and Guam sample crudes and fractions molecular network

| parameter | value |
|---|---|
| workflow version | release_17 |
| PAIRS_MIN_COSINE | 0.7 |
| ANALOG_SEARCH | 1 |
| tolerance.PM_tolerance | 1.0 |
| tolerance.Ion_tolerance | 0.5 |
| MIN_MATCHED_PEAKS | 4 |
| TOPK | 10 |
| CLUSTER_MIN_SIZE | 2 |
| MAXIMUM_COMPONENT_SIZE | 100 |
| MIN_PEAK_INT | 0.0 |
| FILTER_STDDEV_PEAK_INT | 0.0 |
| RUN_MSCLUSTER | on |
| FILTER_PRECURSOR_WINDOW | 1 |
| FILTER_LIBRARY | 1 |
| WINDOW_FILTER | 1 |
| SCORE_THRESHOLD | 0.7 |
| MIN_MATCHED_PEAKS_SEARCH | 4 |
| MAX_SHIFT_MASS | 100.0 |

356

357 **Table S12.** VLC fractionation solvent systems

| fraction | composition |
|---|---|
| A | 100% hexane |
| B | 90% hexane : 10% ethyl acetate |
| C | 80% hexane : 20% ethyl acetate |
| D | 60% hexane : 40% ethyl acetate |
| E | 40% hexane : 60% ethyl acetate |
| F | 20% hexane : 80% ethyl acetate |
| G | 100% ethyl acetate |
| H | 75% ethyl acetate : 25% methanol |
| I | 100% methanol |

358

359

360

361

362

363

364 **Table S13.** $^{1}H$ and $^{13}C$ NMR Data for doscadenamide A (**1**) in $CDCl_3$[a]

| Residue | Position | $\delta_C$, type | $\delta_H$, mult. ( *J*, Hz ) |
|---|---|---|---|
| **pyLys-OMe** | 1 | 170.0, C | |
| | 2 | 94.2, CH | 5.04, s |
| | 3 | 179.2, C | |
| | 4 | 59.2, CH | 4.64, dd (*J* = 5.7, 2.9 Hz) |
| | 5 | 29.0, $CH_2$ | 2.07, m<br>1.84, m |
| | 6 | 20.4, $CH_2$ | 1.19, m<br>1.16, m |
| | 7 | 29.6, $CH_2$ | 1.44, m |
| | 8 | 39.3, $CH_2$ | 3.22, dp (*J* = 19.2, 6.4 Hz)<br>3.13, dp (*J* = 19.2, 6.4 Hz) |
| | 9 | 58.9, $CH_3$ | 3.84, s |
| | NH | | 5.53, brs |
| **Moya-1** | 10 | 177.0, C | |
| | 11 | 41.8, CH | 2.13, m |
| | 12 | 33.9, $CH_2$ | 1.62, m<br>1.35, m |
| | 13 | 28.5, $CH_2$ | 1.36, m |
| | 14 | 28.5, $CH_2$ | 1.50, m |
| | 15 | 18.5[b], $CH_2$ | 2.18, m |
| | 16 | 84.7, C | |
| | 17 | 68.52[c], CH | 1.934[b], t ( *J* = 2.7 Hz) |
| | 18 | 18.1[d], $CH_3$ | 1.11, d (*J* = 1.1 Hz) |
| **Moya-2** | 19 | 176.4, C | |
| | 20 | 39.1, CH | 3.75, m |
| | 21 | 33.7, $CH_2$ | 1.75, m<br>1.42, m |
| | 22 | 26.7, $CH_2$ | 1.39, m |
| | 23 | 26.4, $CH_2$ | 1.44, m |
| | 24 | 18.4[b], $CH_2$ | 2.18, m |
| | 25 | 84.6, C | |
| | 26 | 68.50[c], CH | 1.940[b], t (*J* = 2.7 Hz) |
| | 27 | 16.3[d], $CH_3$ | 1.12, d (*J* = 1.1 Hz) |

365 [a] Data recorded at 600 MHz ($^{1}H$ NMR) and 125 MHz ($^{13}C$ NMR). [b,c,d] Assignments with the same superscripted letter could be
366 reversed.
367



368